Accepted Manuscript

Design, synthesis and biological evaluation of hydroxypyridinone-coumarin hybrids as multimodal monoamine oxidase B inhibitors and iron chelates against Alzheimer's disease

Changjun Zhang, Ke Yang, Sihang Yu, Jing Su, Shengli Yuan, Jiaxin Han, Yan Chen, Jinping Gu, Tao Zhou, Renren Bai, Yuanyuan Xie

PII: S0223-5234(19)30652-X

DOI: https://doi.org/10.1016/j.ejmech.2019.07.031

Reference: EJMECH 11528

To appear in: *European Journal of Medicinal Chemistry*

Received Date: 23 June 2019

Revised Date: 9 July 2019

Accepted Date: 9 July 2019

Please cite this article as: C. Zhang, K. Yang, S. Yu, J. Su, S. Yuan, J. Han, Y. Chen, J. Gu, T. Zhou, R. Bai, Y. Xie, Design, synthesis and biological evaluation of hydroxypyridinone-coumarin hybrids as multimodal monoamine oxidase B inhibitors and iron chelates against Alzheimer's disease, *European Journal of Medicinal Chemistry* (2019), doi: https://doi.org/10.1016/j.ejmech.2019.07.031.

Graphic abstract

Design, synthesis and biological evaluation of hydroxypyridinone-coumarin hybrids as multimodal monoamine oxidase B inhibitors and iron chelates against Alzheimer's disease

Changjun Zhang [a, #], Ke Yang [b, #], Sihang Yu [c], Jing Su [c], Shengli Yuan [b], Jiaxin Han [b], Yan Chen [b], Jinping Gu [b], Tao Zhou [d], Renren Bai [b, *], Yuanyuan Xie [a, b, *]

[a]Collaborative Innovation Center of Yangtze River Delta Region Green Pharmaceutical, Zhejiang University of Technology, Hangzhou, China

[b]College of Pharmaceutical Science, Zhejiang University of Technology, Hangzhou, China

[c]Department of Pathophysiology, College of Basic Medical Sciences, Jilin University, Changchun, China

[d]School of Food Science and Biotechnology, Zhejiang Gongshang University, Hangzhou, China

[#]These authors contributed equally to this work

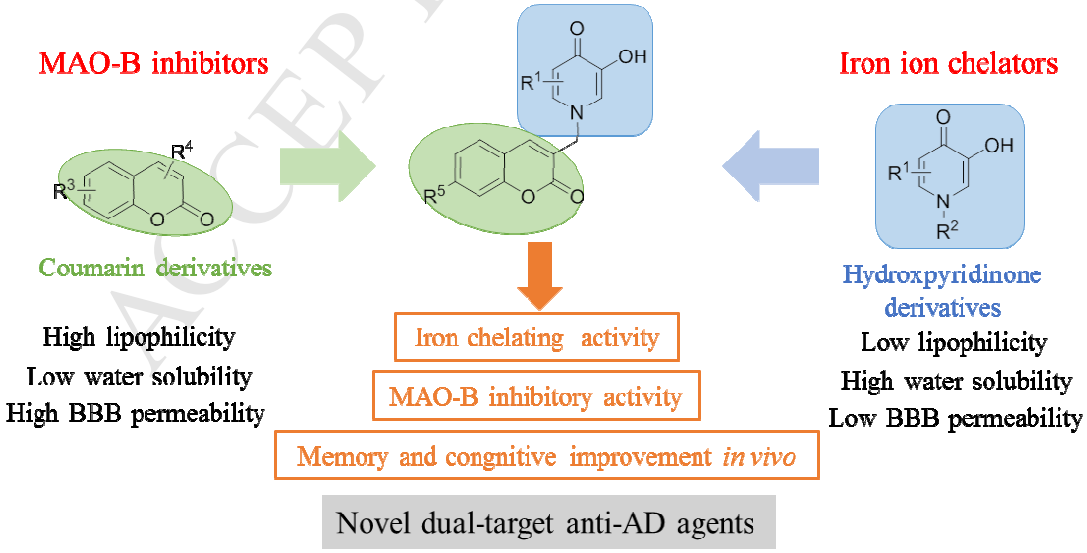

Design, synthesis and biological evaluation of hydroxypyridinone-coumarin hybrids as multimodal monoamine oxidase B inhibitors and iron chelates against Alzheimer's disease

Changjun Zhang [a, #], Ke Yang [b, #], Sihang Yu [c], Jing Su [c], Shengli Yuan [b], Jiaxin Han [b], Yan Chen [b], Jinping Gu [b], Tao Zhou [d], Renren Bai [b, *], Yuanyuan Xie [a, b, *]

[a]Collaborative Innovation Center of Yangtze River Delta Region Green Pharmaceutical, Zhejiang University of Technology, Hangzhou, China

[b]College of Pharmaceutical Science, Zhejiang University of Technology, Hangzhou, China

[c]Department of Pathophysiology, College of Basic Medical Sciences, Jilin University, Changchun, China

[d]School of Food Science and Biotechnology, Zhejiang Gongshang University, Hangzhou, China

[#]These authors contributed equally to this work

Correspondence:

Dr. Yuanyuan Xie, Key Laboratory for Green Pharmaceutical Technologies and Related Equipment of Ministry of Education, College of Pharmaceutical Science, Zhejiang University of Technology, Hangzhou 310014, China. Email: xyycz@zjut.edu.cn

Dr. Renren Bai, College of Pharmaceutical Science, Zhejiang University of Technology, Hangzhou 310014, China. Email: renrenbai@zjut.edu.cn

Abstract

A series of hybrids of hydroxypyridinone and coumarin were rationally designed, synthesized and biologically evaluated for their iron ion chelating and MAO-B inhibitory activities. Most of the compounds displayed excellent iron ion chelating effects and moderate to good anti-MAO-B activities. Compound **27a** exhibited the most potent activity against MAO-B, with an IC_{50} value of 14.7 nM. Importantly, **27a** showed good U251 cell protective effect and significantly ameliorated the cognitive dysfunction of scopolamine-induced AD mice. Moreover, molecular docking was performed to elucidate the probable ligand-receptor interaction, and the structure-activity relationships were also summarized.

Keywords: Alzheimer's disease; Iron ion chelator; MAO-B inhibitor; Coumarin derivatives; Hydroxypyridinones

1. Introduction

Alzheimer's disease (AD) is a typical progressive neurodegenerative disorder characterized by dementia, cognitive impairment, and memory loss [1]. Although it has been discovered more than 100 years, the etiology of AD remains ambiguous. The accumulative formation of β-amyloid (Aβ) deposits, hyper-phosphorylated τ-protein aggregation, oxidative stress, dyshomeostasis of biometals, and low levels of acetylcholine (ACh) are considered to play crucial roles in the pathogenesis of AD [2-4]. To date, the therapeutic options for AD patients were limited within one *N*-methyl-*D*-aspartate (NMDA) receptor antagonist (Memantine) and three acetylcholinesterase (AChE) inhibitors (Donepezil, Rivastigmine and Galantamine). However, the therapeutic effects are limited due to the multifactorial and complex nature of AD [5].

In recent years, monoamine oxidases (MAOs), the important enzymes involved

in monoamine neurotransmitters metabolism and oxidative stress, have received increasing attention for their potential roles in the treatment of AD [6, 7]. MAOs are flavin adenine dinucleotide (FAD)-containing enzymes that are responsible for the oxidative deamination of various biogenic and dietary amines. MAO-B is one of the enzymatic isoforms, which accelerates the oxidative deamination of β-phenethylamine and benzylamine [8, 9]. MAO-B inhibitors are employed to treat neurodegenerative diseases. For example, safinamide is a well-known MAO-B inhibitor recently approved for Parkinson's therapy [10]. The oxidative deamination catalyzed by MAO-B leads to the higher levels of neurotoxic products, such as hydrogen peroxide and aldehydes, which promote the formation of reactive oxygen species (ROS) and may contribute to neuronal damage [11, 12]. Studies have shown that MAO-B expression in neuronal tissues increases 4-fold in the elderly, and its activity elevated in brains of AD patients increases the rate of neurotransmitters consumption and neuronal damage [8, 13]. Meanwhile, evidence has shown that MAO-B inhibitors can significantly improve learning memory deficits in animal models due to the inhibition of the oxidative stress in AD [14]. Overall, these observations suggest that MAO-B inhibitors demonstrate great potential for the treatment of AD.

The dyshomeostasis of brain metal-ion is one of the important hallmarks of AD, related to the formation of both amyloid plaques and neurofibrillary tangles [15-17]. Recently, studies found that transition metals, especially for iron and copper ions, bind to amyloid plaques directly, which suggests that overloaded metal ions in the neuropil and plaques of the brain closely associated with the formation of Aβ plaques and neurofibrillary tangles [18]. Additionally, the high concentration of redox-active metal ions might work as a catalyst involved in the production of reactive oxygen species (ROS), resulting in oxidative stress [19]. Thus, chelating agents have been proposed as a potential therapeutic option for the treatment of AD by modulating the level of biometals in the brain [20, 21].

On the account of the insufficiency of traditional “one drug, one target” therapy methods, the multi-target-directed ligand (MTDL) strategy based on the “one molecule, multiple target” paradigm has been developed by acting on multitarget

simultaneously for the efficient treatment of the multifaceted disease [5, 22]. In view of the importance of MAO-B, biometals, and oxidative stress in the treatment of AD, designing MTDLs with MAO-B inhibition, iron chelation, and antioxidative ability received much attention in recent years [23, 24]. Previously, we reported the rapid construction of dual-target anti-Alzheimer's disease agents with both iron ion chelating and MAO-B inhibitory activity by click chemistry, and most of the compounds showed efficient iron ion chelating ability and favorable MAO-B inhibitory activity [25]. Inspired by these drug design strategies, in this work, we designed a novel series of hydroxypyridinone-coumarin hybrids as multimodal monoamine oxidase-B inhibitors and iron chelates against AD.

2. Results and discussion

2.1. Design of the hydroxypyridinone-coumarin hybrids

Researchers have demonstrated that coumarin is one of the most privileged scaffolds of MAO-B, and the structure-activity relationships (SARs) of coumarin derivatives, especially for 3-phenyl, and 7-benzyloxy substituted derivatives have been comprehensively investigated [26-29]. Therefore, the planar coumarin scaffold was chosen and the C-7 of coumarin ring was modified to enhance the anti-MAO-B efficacy as well as promote the selectivity over MAO-A [30-35].

Deferiprone is a widely used iron-selective chelator for the treatment of systemic iron overload, which can effectively chelate oxidative iron$^{(III)}$ from the iron-overloaded tissues without disturbing the normal cytosolic labile iron pool [15, 36]. Coumarin derivatives usually show high lipophilicity, resulting in preferable membrane penetrating ability, but their water solubility is poor. While hydroxypyridinone derivatives possess excellent water solubility but display low membrane penetrating ability and bioavailability [17]. Overall, the rational combination of hydroxypyridinone and coumarin is a promising strategy for the treatment of neurodegenerative diseases.

Based on the multitarget directed ligand strategy, a novel molecular framework was rationally designed by integrating the structures of hydroxypyridin-4-one groups

with C-7 substituted coumarin derivatives.

(Fig. 1)

2.2. Chemistry

The synthesis of the novel hybrids **8a-c**, **13a-c**, and **24-29**(**a-c**) are depicted in **Schemes 1** to **3**. Intermediates **3a** to **3c** were easily prepared from market available precursors maltol, ethyl maltol, and 5-hydroxy-2-methyl-4*H*-pyran-4-one, respectively (**Scheme 1**). The protection of hydroxyl groups at the pyrone rings of **1a-c** provided the methyl or benzyl protected derivatives **2a-c**. Subsequently, the ring oxygen was substituted by nitrogen via reaction with ammonium hydroxide to obtain the corresponding pyridinone derivatives **3a-c** [37]. Coumarin derivatives were prepared following the reported methods via reaction of propionic anhydride with benzaldehyde **4**, **9**, and **14** respectively, to afford intermediates **5**, **10**, and **15** [38]. Then, the 3-methyl moiety was substituted with the bromomethyl group to give 3-bromomethyl coumarin **6**, **11**, **16** [39].

According to S**cheme 2** and **3**, coumarin-based hybrids **7a-c**, **12a-c**, **18 a-c**, and **23a-c** were synthesized by a nucleophilic substitution reaction between the pyridin-4(1*H*)-one (**3a-3c**) and 3-bromomethyl coumarin. The desired compounds **8a-c** and **13a-c** were obtained via demethylation of **7a-c**, **12a-c** by treatment with boron tribromide (BBr_3). In terms of compounds **24-29**(**a-c**), the gathered intermediates **17a-c** were refluxed in 50% acetone-water solution, subsequently treated with propargyl bromide or corresponding benzyl bromide in the presence of potassium carbonate to afford the key intermediate **18-23(a-c)**. Then the protecting group of pyridinone moiety was selectively removed to obtain the final compounds.

(**Scheme 1**)

(**Scheme 2**)

(**Scheme 3**)

2.3. Acid dissociation constants and iron$^{(III)}$ affinity constants test of the hybrids

An automated spectrophotometric titration system was applied to test the pK_a and logK_{eq} (Fe^{3+}) values [36, 40]. The determined pK_a values and affinity constants for iron$^{(III)}$ are presented in **Table 1**. Most of the compounds showed the promising pFe^{3+} chelating effect with pFe^{3+} values around 18. Compounds **26c** and **28a**, displayed the most potent chelating activity with pFe^{3+} values of 18.75 and 18.65, respectively, superior to that of the reference drug deferiprone (pFe^{3+} = 17.26). Thus, in general, all the hybrids inherited the excellent iron chelating ability of the deferiprone pharmacophore.

(**Table 1**)

(**Scheme 4**)

For all of the synthesized compounds, the UV profiles yielded two pK_a values. The lower pK_{a1} value (< 3.26) is assigned to the protonation of the 4-oxo group and the higher pK_{a2} value in the range of 8.87-9.76 is assigned to the dissociation of 3- (or 5-) hydroxyl group (**Scheme 4**) [41]. Since the acid dissociation constant was evaluated in a saline system, the detected p*K*a values indicate the remarkable enhancement of water solubility of the parent coumarin structure. The UV profile of **27a** over the pH range of 2.0-10.5 (**Fig. 2**) yielded two pK_a values, 3.10 and 9.65, respectively. When the titration was proceeded in the presence of iron$^{(III)}$, over the pH range of 1.2-8.0, the visible profile was indicative of three species, FeL, FeL_2, and FeL_3 (**Fig. 3**) [42]. Resolution of the spectra of these three species led to the determination of the corresponding three affinity constants: logK_1 (14.26), logK_2 (25.32) and logK_3 (34.25). The pFe^{3+} value (18.04) was then calculated based on the above three affinity constants. It is obvious that under most physiological conditions, the dominant species is the neutral $Fe^{III}L_2$ complex, even when the iron$^{(III)}$ and **27a** concentrations are below the micromolar level [41]. Comparatively, both pK_a values of the hybrids are lower than the corresponding value of deferiprone, resulting from the delocalization of the negative charge on 4-oxygen across the ring to the ring nitrogen

cation (**Scheme 4**).

(Fig. 2)

(Fig. 3)

2.4. Discussion

The MAO-B inhibitory activities of all the targeted compounds were preliminarily evaluated at 10 μM and pargyline (a MAO-B inhibitor) was selected as the reference drug. As shown in **Table 2**, most of the compounds exhibited significant MAO-B inhibitory effect at the concentration of 10 μM. Subsequently, compounds with favorable anti-MAO-B activity (more than 75% inhibition) were submitted to the following IC_{50} test (**Table 3**). As illustrated in **Table 2** and **3**, although the hydroxypyridinone moiety was introduced to the parent structure of coumarin, the obtained hybrids successfully maintained the inhibitory activity against MAO-B, and there are slight differences among the three chemical series of hydroxypyridinones. In general, compounds modified at C-7 of the coumarin ring exhibited better MAO-B inhibitory activities, with IC_{50} values ranging from submicromolar to lower nanomolar concentrations. Compound **27a** was proved to be the most potent hybrid displaying the highest MAO-B inhibitory activity (IC_{50} = 14.7 nM), which was even more efficient than that of pargyline (IC_{50} = 85.8 nM). Compounds **8a-c** were approximately two-fold less potent than that of the methoxyl (**13a-c**) and propargyl (**24a-c**) substituted hybrids at the side chain of C-7. Moreover, it was obvious that with the lengthen and the substitution group such as benzyloxy resulted in remarkable potency enhancement. Additionally, after the introduction of electron-withdrawing groups (Cl and F) at meta- or para-position of the benzyloxy phenyl ring, the obtained hybrids exhibited better MAO-B inhibition. Interestingly, compound **13a** showed a lower IC_{50} value of 91.9 nM.

(**Table 2**)

(**Table 3**)

2.5.Molecular modeling

In order to elucidate the probable binding modes, docking simulations were performed using the CDOCKER program of the Discovery Studio 2016 software. The X-ray crystal structure of human MAO-B (PDB entry 2v5z) was used acquired from the PDB [43]. Based on the *in vitro* inhibitory results, compounds **13a** and **27a** were selected as typical ligands for the evaluation. As shown in **Fig. 4**, several lipophilic interactions anchoring the coumarin moiety of the hybrids at the aromatic substrate cavity of both **13a** and **27a**, and the hydroxypyridinone moiety was toward the FAD cofactor. The binding mode showed important interactions between hydroxypyridinone moiety and residues around it, which indicated that hydroxypyridinone moiety, not only rendering chelating ability but also worked as a key fragment in binding with MAO-B. There were two hydrogen bonds between furan-carbonyl oxygen and the residues GLN 206 and TYR 326. These interactions, in part, might explain the good inhibitory activity of **13a**. In the case of **27a**, the ligand crossed both the entrance and substrate cavities of the enzyme. The C-7 3-F-benzyloxy of compound **27a** occupied the hydrophobic entrance cavity of the enzyme and interacted with the lipophilic residues ILE 199, ILE 316, LEU 164, PRO 104 and PHE 103. Besides, the fluorine atom established a halogen interaction with residue PRO102. Moreover, the hydroxyl of pyridinone formed a hydrogen bond with residue GLN 206, and Pi-alkyl interaction was observed between the methyl of pyridinone and TYR 435 as well as FAD. Those observations might explain the best activity of the **27a**.

(Fig. 4)

2.6.Cytotoxicity and cytoprotective effects of the compound 27a on U251 cells.

The safety is important for the CNS drugs, so the potential toxic effect of **27a** was investigated on human glioma cell line U251. The cells were exposed to compound **27a** at the concentration of 10 nM, 1 μM, and 100 μM respectively for 24

h and the cell viability was determined by the MTS assay [44, 45]. As shown in **Fig. 5A**, compound **27a** showed no cytotoxicity even at the concentration of 100 μM.

Meanwhile, we evaluated the cytoprotective effects of compound **27a** on H_2O_2-induced cell damage (**Fig. 5B**) [35]. Treatment with 100 μM H_2O_2 for 1 h resulting in over 50% death of U251 cells. When cells pretreated with **27a** (100 μM) for 24 h, the cell viability increased to 57.8 ± 3.9%, close to that of pargyline (100 μM, 61.5 ± 4.7%) or vitamin C (100 μM, 57.6 ± 3.5%) pretreated group. These results indicated that **27a** had cytoprotective activity against antagonizing oxidative stress.

(Fig. 5)

2.7. Behavioral studies

The improvement of cognitive ability is of great importance for the development of anti-AD agents. Based on the multiple evaluations mentioned above, **27a** showed the best multipotent activity and was selected for *in vivo* behavioral study by using a Morris water maze test [46].

Scopolamine was selected to build the cognition-impaired adult ICR mice animal model, which was applied for the behavioral evaluation of **27a**. Pargyline (10 $mg \cdot kg^{-1}$) was used as a reference drug. 30 min before the intraperitoneal administration of scopolamine (1 $mg \cdot kg^{-1}$) or blank solution, **27a** and pargyline were intraperitoneally injected to the ICR mice for two consecutive weeks to adapt the apparatus. The test included 2 days of learning and memory training, followed by a probe trial on the fifth day. For all of the groups, the data on the fifth day was presented in mean ± SEM and are shown in **Table 4** and **Fig. 6**.

Compared to the control group, scopolamine led to a remarkable delay of the latency to target (15.3 ± 1.2 seconds vs. 40.2 ± 10.5 seconds, $^{\#}p < 0.05$), indicating that the cognitive impairment mouse model was successfully built. For the pargyline treated group, the latency to target reduced to 5.6 ± 2.0 seconds ($^{*}p < 0.05$), showing pargyline could ameliorate the impairment. Compared to the control group, animals treated with compound **27a** resulted in a significant reduction in the latency to target

(9.6 ± 3.4 seconds, *p < 0.05), which demonstrated that **27a** considerably ameliorated the cognitive impairment of the mice with comparable efficacy to pargyline. From this observation, we can roughly conclude that **27a** could penetrate the blood-brain barrier (BBB) and target the MAO-B in the central nervous system (CNS).

The distance of the mice motion track to the target (**Table 4** and **Fig. 6B**) and the the times that mice entered the target quadrant (**Table 4** and **Fig. 6C**) were also analyzed. Compared to the control group, administration of scopolamine significantly led to the extended distance of the mice motion track (10.4 ± 1.2 m vs. 5.8 ± 0.7 m, $^{\#\#}p < 0.005$). Moreover, the enter target quadrant times were markedly decreased (16.5 ± 0.8 vs. 9.0 ± 0.8, $^{\#\#\#}p < 0.001$). Pargyline slightly shortened the distance to target (6.6 ± 0.6 m, $^{*}p < 0.05$). When treated with compound **27a**, the distance to target was remarkably shortened (4.2 ± 0.6 m, ***p < 0.001). Compared to the control group, both pargyline and **27a** increased the times enter target quadrant of the mice, even close to a normal level (16.3 ± 1.5, ***p< 0.001, 16.6 ± 0.8, ***p< 0.001, respectively). These results were also supported by trajectory analysis. As shown in **Fig. 6B**, the trajectories of the mice in scopolamine model group was very long and in a muddle, while **27a** and pargyline groups (**Fig. 6C** and **D**) displayed a shortened track (**Fig. 6A**). Taken together, these results supported that **27a** remarkably ameliorated the cognition impairment caused by scopolamine.

(**Table 4**)

(Fig. 6)

3. Conclusion

In summary, a novel series of hydroxypyridinone-coumarin hybrids were designed and prepared by pharmacophore fusion strategy, acting as multi-target-directed agents for the treatment of Alzheimer's disease. The designed compounds showed promising anti-MAO-B activities and biometal chelating effects in the *in vitro* assays. Compound **27a** was proved to be the most effective MAO-B inhibitor (IC_{50} = 14.7 nM), superior to that of the reference drug pargyline (IC_{50} =

85.8 nM). The molecular docking analysis demonstrated that **27a** could bind to both the entrance cavity and the substrate cavity of MAO-B. Additionally, compound **27a** displayed cytoprotective activity against oxidative stress and could significantly ameliorate the cognition impairment in a Morris water maze test model. The present study indicates that **27a** is a promising multifunctional agent with potential anti-AD activity, and the design of dual MAO-B inhibitor and iron ion chelator is a useful strategy for the treatment of AD.

4. Experimental section

4.1. General information

All starting materials and reference compounds were obtained from commercial sources without further purification. The ^{1}H NMR and ^{13}C NMR spectra were recorded on a Bruker BioSpin GmbH spectrometer (Bruker, Germany) at 600 and 150 MHz respectively, where $CDCl_3$ or DMSO-d_6 was used as the solvent. Tetramethylsilane was used as standard and chemical shifts are reported in parts per million (ppm), coupling constants *J* are given in Hertz (Hz), and spin multiplicities are given as singlet (s), broad singlet (br s), doublet (d), doublet of doublets (dd), doublet of doublets of doublets (ddd), triplet (t), doublet of triplets (dt), quartet (q), and multiplet (m). Electrospray ionization mass spectrometry (ESI-MS) was performed on an amazon speed (Bruker, Germany) in positive polarity. Data were listed as mass number ($[M+H]^+$) and relative intensity (%). High-resolution mass spectra were obtained using a Shimadzu LCMS-IT-TOF mass spectrometer. Melting points (m.p., uncorrected) were determined on a M-564 Büchi melting point apparatus (Büchi, Germany). All the reactions were routinely monitored by thin layer chromatography on silica gel and visualized using UV light (254 nm light source).

4.2. General procedure for the preparation of compounds 3a-3c.

A mixture of suitable Maltol (7.56 g, 60 mmol), anhydrous K_2CO_3 (9.12 g, 66 mmol), benzyl bromide (10.78 g, 63 mmol) and acetone (150 mL) was refluxed for 8 h. Once the reaction was completed, the mixture was cooled to room temperature.

After the solvent was removed under reduced pressure, water (100 mL) was added and the mixture was extracted four times with dichloromethane (50 mL). The combined organic layer was dried over anhydrous sodium sulfate and the solvent was removed under reduced pressure to afford intermediate **2a** as yellow oil. Intermediates **2b**, **2c** wasprepared followed the similar procedure of **2a**. **2a**, **2b** or **2c** (4.33 g, 40 mmol) was then dissolved in ethanol 45 mL and then 25% ammonia aqueous solution (60 mL) was added, and the mixture was refluxed for 12 h. Afterward, The solvent was evaporated off to obtain a pale brown solid residue, which was recrystallized from acetone/ ethyl acetate, leaving the pure target compound as a pale colored solid.

4.2.1. 3-Methoxy-2-methylpyridin-4(1*H*)-one (**3a**[1])

Yield: 75%, m.p. = 154.8°C, ^{1}H NMR (600 MHz, Chloroform-d), δ (ppm): 13.50 (s, 1H), 7.52 (d, *J* = 7.1, 0.9 Hz, 1H), 6.44 (d, *J* = 7.0, 1.1 Hz, 1H), 3.79 (s, 3H), 2.42 (s, 3H).

4.2.2. 3-(Benzyloxy)-2-methylpyridin-4(1*H*)-one (**3a**[2])

Yield: 82%, m.p. = 123.1°C. ^{1}H NMR (600 MHz, Chloroform-*d*), δ (ppm): 13.38 (s, 1H), 7.42 (d, *J* = 7.0 Hz, 1H), 7.31 - 7.26 (m, 5H), 6.37 (d, *J* = 6.9 Hz, 1H), 5.03 (s, 2H), 2.16 (s, 3H).

4.2.3. 2-Ethyl-3-methoxypyridin-4(1*H*)-one (**3b**[1])

Yield: 73%, m.p. = 148.5°C. ^{1}H NMR (500 MHz, Chloroform-d), δ (ppm): 13.28 (s, 1H), 7.44 (d, *J* = 7.0 Hz, 1H), 6.36 (d, *J* = 6.8 Hz, 1H), 5.09 (s, 2H), 2.69 (q, *J* = 7.2 Hz, 2H), 1.12 (t, *J* = 7.5 Hz, 3H).

4.2.4. 3-(Benzyloxy)-2-ethylpyridin-4(1*H*)-one (**3b**[2])

Yield: 76%, m.p. = 140.7°C. ^{1}H NMR (500 MHz, Chloroform-*d*), δ (ppm): 13.20 (s, 1H), 7.44 (d, *J* = 7.0 Hz, 1H), 7.26 (m, 5H), 6.36 (d, *J* = 6.8 Hz, 1H), 5.09 (s, 2H), 2.60 (q, *J* = 7.5 Hz, 2H), 1.08 (t, *J* = 7.5 Hz, 3H).

4.2.5. 5-Methoxy-2-methylpyridin-4(1*H*)-one (**3c**[1])

Yield: 76%, m.p. = 96.7°C. ^{1}H NMR (600 MHz, DMSO-d6), δ (ppm): 11.29 (s, 1H), 7.28 (s, 1H), 5.98 (s, 1H), 3.63 (s, 3H), 2.17 (s, 3H).

4.2.6. 5-(Benzyloxy)-2-methylpyridin-4(1*H*)-one (**3c**[2])

Yield: 80%, m.p. = 184.3°C. ^{1}H NMR (400 MHz, DMSO-d_6), δ (ppm): 11.21 (s,

1H), 7.9-7.31 (m, 6H), 6.00 (s, 1H), 4.97 (s, 2H), 2.16 (s, 3H).

4.3. General procedure for the preparation of compounds 5, 10 and 15.

A 250 mL round-bottom flask was charged with appropriate salicylaldehyde (60 mmoL), propionic anhydride (23.43 g, 180 mmoL) and sodium propionate (11.53 g, 120 mmoL). Triethylamine (6.07 g, 60 mmoL) was then added, and the recation mixture was refluxed for 10 h. The resulting brown mixture was recrystallized from ethyl acetate (50 mL) afforded a white solid which subsequently was washed by water, obtaining a white product.

4.3.1. 3-Methyl-2*H*-chromen-2-one (**5**)

Yield: 48%, m.p. = 116.5°C. ^{1}H NMR (600 MHz, Chloroform-*d*), δ (ppm): 7.50 (s, 1H), 7.44 (td, *J* = 7.3, 1.3 Hz, 1H), 7.40 (dd, *J* = 7.7, 1.6 Hz, 1H), 7.29 (d, *J* = 8.3 Hz, 1H), 7.24 (td, 1H), 2.20 (s, 3H).

4.3.2. 7-Methoxy-3-methyl-2*H*-chromen-2-one (**10**)

Yield: 45%, m.p. = 117.8°C. ^{1}H NMR (600 MHz, Chloroform-*d*), δ (ppm): 7.45 (s, 1H), 7.30 (d, *J* = 8.3 Hz, 1H), 6.83 - 6.80 (m, 2H), 3.86 (s, 3H), 2.17 (s, 3H).

4.3.3. 3-Methyl-2-oxo-2*H*-chromen-7-yl propionate (**15**)

Yield: 56%, m.p. = 127.3°C. ^{1}H NMR (600 MHz, Chloroform-*d*), δ (ppm): 7.52 - 7.48 (m, 1H), 7.41 (d, *J* = 8.4 Hz, 1H), 7.09 (d, *J* = 2.2 Hz, 1H), 7.01 (dd, *J* = 8.4, 2.2 Hz, 1H), 2.62 (q, *J* = 7.5 Hz, 2H), 2.21 (d, *J* = 1.4 Hz, 3H), 1.28 (t, *J* = 7.5 Hz, 3H).

4.4. General procedure for the preparation of compounds 6, 11 and 16.

To a solution of compound **5** (4.65 g, 20 mmol) in 40 mL of CCl_4 was added NBS (3.74 g, 21 mmol) and a trace amount of BPO (0.1 g), and the mixture was allowed to refluxed for 12 h. After the reaction, 40 mL dichloromethane was added, and the mixture was washed five times with water (60 mL), and the organic layer was dried by anhydrous sodium sulfate. Subsequently, The solvent was evaporated off to afford white colored solid, which was re-crystallized from ethyl acetate/ petroleum, leaving the pure desired product.

4.4.1. 3-(Bromomethyl)-2*H*-chromen-2-one (**6**)

Yield: 75%, m.p. = 120°C. ^{1}H NMR (600 MHz, Chloroform-*d*), δ (ppm): 7.86 (s, 1H), 7.55 (td, 1H), 7.51 (dd, *J* = 7.8, 1.6 Hz, 1H), 7.35 (dd, *J* = 7.8, 0.6 Hz, 1H), 7.31 (td, *J* = 7.5, 1.0 Hz, 1H), 4.44 (s, 2H). ^{13}C NMR (150 MHz, $CDCl_3$), δ (ppm): 161.46, 153.36, 138.76, 131.53, 128.01, 124.79, 119.22, 116.78, 61.27, 29.84.

4.4.2. 3-(Bromomethyl)-7-methoxy-2*H*-chromen-2-one (**11**)

Yield: 52%, m.p. = 133.0°C. ^{1}H NMR (600 MHz, Chloroform-*d*), δ (ppm): 7.79 (s, 1H), 7.39 (d, *J* = 8.6 Hz, 1H), 6.86 (dd, *J* = 8.6, 2.4 Hz, 1H), 6.82 (d, *J* = 2.4 Hz, 1H), 4.42 (s, 2H), 3.88 (s, 3H). ^{13}C NMR (150 MHz, $CDCl_3$), δ (ppm): 163.32, 160.39, 155.82, 142.31, 129.17, 121.87, 113.17, 112.62, 100.79, 55.99, 28.30.

4.4.3. 3-(Bromomethyl)-2-oxo-2*H*-chromen-7-yl propionate (**16**)

Yield: 95%, m.p. = 118.3°C. ^{1}H NMR (600 MHz, Chloroform-d), δ (ppm): 7.84 (s, 1H), 7.50 (d, *J* = 8.5 Hz, 1H), 7.13 (d, *J* = 2.2 Hz, 1H), 7.07 (dd, *J* = 8.5, 2.2 Hz, 1H), 4.42 (s, 2H), 2.63 (q, *J* = 7.6 Hz, 2H), 1.28 (t, *J* = 15.1 Hz, 3H). ^{13}C NMR (100 MHz, $CDCl_3$), δ (ppm): 172.19, 159.64, 154.34, 153.55, 141.45, 128.79, 124.82, 118.82, 116.59, 110.28, 27.75, 27.56, 8.92.

4.5. General procedure for the preparation of compounds 7a-c, 12a-c, 17a-c.

A mixture of **6** (239 mg, 1.5 mmol), **3a**[1] (139 mg, 1.0 mmol), anhydrous potassium carbonate (207 mg, 1.5 mmol), and acetonitrile (15 mL) was refluxed for 6 h, and the progress of the reaction was monitored by TLC (eluent: dichloromethane/ methanol = 15: 1 solvent mixture). The reaction mixture was concentrated under reduce pressure to afford yellow solid residue, which was purified by chromatography on silica gel to obtain the desired compound.

4.5.1. 3-(Methyloxy)-2-methyl-1-((2-oxo-2*H*-chromen-3-yl) methyl) pyridin-4(1*H*)-one (**7a**)

Yield: 55%, m.p. = 192.0°C. ^{1}H NMR (600 MHz, DMSO-d_6), δ (ppm): 7.76 (dd, *J* = 7.8, 1.5 Hz, 1H), 7.69 (d, *J* = 7.6 Hz, 1H), 7.61 (ddd, *J* = 8.5, 7.4, 1.6 Hz, 1H), 7.48 (s, 1H), 7.43 (d, *J* = 8.3 Hz, 1H), 7.34 (td, *J* = 7.5, 1.0 Hz, 1H), 6.19 (d, *J* = 7.5 Hz, 1H), 5.02 (d, *J* = 1.5 Hz, 2H), 3.71 (s, 3H), 2.27 (s, 3H). ^{13}C NMR (150 MHz, DMSO), δ (ppm): 172.08, 159.45, 152.68, 146.94, 140.73, 140.04, 138.83, 131.90, 128.68, 124.68, 124.35, 118.64, 116.37, 116.03, 58.55, 51.69, 11.76. HRMS m/z: calc.

for $C_{17}H_{15}NO_4Na$ $[M+Na]^+$, 320.0893, found 320.0903.

4.5.2. 3-(Methyloxy)-2-ethyl-1-((2-oxo-2*H*-chromen-3-yl) methyl) pyridin-4(1*H*)-one (**7b**)

Yield: 33%, m.p. = 193.1°C. ^{1}H NMR (600 MHz, Chloroform-*d*), δ (ppm): 7.56 (ddd, *J* = 8.6, 7.3, 1.6 Hz, 1H), 7.44 (dd, *J* = 7.7, 1.5 Hz, 1H), 7.36 (d, *J* = 8.3 Hz, 1H), 7.31 (td, *J* = 7.5, 1.1 Hz, 2H), 7.03 (d, *J* = 1.7 Hz, 1H), 6.52 (d, *J* = 7.5 Hz, 1H), 4.96 (d, *J* = 1.6 Hz, 2H), 3.96 (s, 3H), 2.68 (t, *J* = 7.5 Hz, 2H), 1.22 (t, *J* = 7.5 Hz, 3H). ^{13}C NMR (150 MHz, $CDCl_3$), δ (ppm): 173.85, 159.88, 153.26, 147.99, 145.67, 139.03, 138.76, 132.54, 128.37, 125.22, 124.40, 118.39, 118.36, 116.83, 60.01, 51.85, 19.97, 14.03. HRMS m/z: calc. for $C_{18}H_{18}NO_4$ $[M+H]^+$, 312.1230, found 312.1217.

4.5.3. 5-(Methyloxy)-2-methyl-1-((2-oxo-2*H*-chromen-3-yl) methyl) pyridin-4(1*H*)-one (**7c**)

Yield: 52%, m.p. = 257.1°C. ^{1}H NMR (600 MHz, Chloroform-*d*), δ (ppm): 7.57 (ddd, *J* = 8.7, 7.4, 1.6 Hz, 1H), 7.46 (dd, *J* = 7.8, 1.6 Hz, 1H), 7.36 (d, *J* = 8.3 Hz, 1H), 7.32 (td, *J* = 7.5, 1.1 Hz, 1H), 7.06 (d, *J* = 1.6 Hz, 1H), 7.01 (s, 1H), 6.39 (s, 1H), 4.93 (d, *J* = 1.7 Hz, 2H), 3.78 (s, 3H), 2.27 (s, 3H). ^{13}C NMR (150 MHz, $CDCl_3$), δ (ppm): 172.91, 159.96, 153.27, 150.14, 145.51, 138.71, 132.57, 128.38, 125.24, 123.77, 122.61, 118.39, 117.52, 56.47, 52.18, 19.16. HRMS m/z: calc. for $C_{17}H_{16}NO_4$ $[M+H]^+$, 298.1070, found 298.1074.

4.5.4. 3-(Methyloxy)-1-((7-methoxy-2-oxo-2*H*-chromen-3-yl)methyl)-2-methylpyridin-4(1*H*)-one (**12a**)

Yield: 48%, m.p. = 174.0°C. ^{1}H NMR (600 MHz, Chloroform-*d*), δ (ppm): 7.33 (dd, *J* = 8.1, 5.8 Hz, 2H), 7.03 (d, *J* = 1.6 Hz, 1H), 6.87 (dd, *J* = 8.7, 2.4 Hz, 1H), 6.83 (d, *J* = 2.4 Hz, 1H), 6.49 (d, *J* = 7.5 Hz, 1H), 4.91 (d, *J* = 1.5 Hz, 2H), 3.89 (s, 3H), 3.87 (s, 3H), 2.33 (s, 3H). ^{13}C NMR (150 MHz, $CDCl_3$), δ (ppm): 173.72, 163.45, 160.31, 155.22, 148.38, 140.60, 139.11, 139.04, 129.31, 119.85, 118.07, 113.32, 112.02, 100.88, 59.76, 56.03, 52.41, 12.40. HRMS m/z: calc. for $C_{18}H_{18}NO_5$ $[M+H]^+$, 328.1179, found 328.1182.

4.5.5. 3-(Methyloxy)-2-ethyl-1-((7-methoxy-2-oxo-2*H*-chromen-3-yl)methyl)pyridin-4(1*H*)-one(**12b**)

Yield: 49%, m.p. = 177.4°C. ^{1}H NMR (600 MHz, Chloroform-*d*), δ (ppm): 7.34 (d, *J* = 8.7 Hz, 2H), 7.06 (s, 1H), 6.87 (dd, *J* = 8.7, 2.4 Hz, 1H), 6.82 (d, *J* = 2.4 Hz, 1H), 6.53 (d, *J* = 7.5 Hz, 1H), 4.94 (d, *J* = 1.5 Hz, 2H), 3.96 (s, 3H), 3.87 (s, 3H), 2.70 (q, *J* = 7.5 Hz, 2H), 1.22 (t, *J* = 7.5 Hz, 3H). ^{13}C NMR (150 MHz, $CDCl_3$), δ (ppm): 173.60, 163.44, 160.32, 155.19, 147.84, 146.07, 139.28, 139.16, 129.40, 120.24, 118.10, 113.29, 112.04, 100.87, 60.05, 56.02, 51.88, 19.98, 14.00. HRMS m/z: calc. for $C_{19}H_{20}NO_5$ $[M+H]^+$, 342.1336, found 342.1347.

4.5.6. 5-(Methyloxy)-1-((7-methoxy-2-oxo-2*H*-chromen-3-yl)methyl)-2-methylpyridin-4(1*H*)-one (**12c**)

Yield: 72%, m.p. = 195.3°C. ^{1}H NMR (600 MHz, Chloroform-*d*), δ (ppm): 7.37 (d, *J* = 8.6 Hz, 1H), 7.14 (s, 1H), 7.11 (s, 1H), 6.88 (dd, *J* = 8.7, 2.4 Hz, 1H), 6.83 (d, *J* = 2.4 Hz, 1H), 6.43 (s, 1H), 4.94 (d, *J* = 1.4 Hz, 2H), 3.88 (s, 3H), 3.79 (s, 3H), 2.31 (s, 3H). ^{13}C NMR (150 MHz, $CDCl_3$), δ (ppm): 172.26, 163.50, 160.46, 155.29, 149.85, 145.83, 139.57, 129.44, 123.08, 119.60, 117.30, 113.32, 112.06, 100.89, 56.63, 56.04, 52.31, 19.33. HRMS m/z: calc. for $C_{18}H_{18}NO_5$ $[M+H]^+$, 328.1179, found 328.1167.

4.5.7. 3-((3-(Benzyloxy)-2-methyl-4-oxopyridin-1(4*H*)-yl)methyl)-2-oxo-2*H*-chromen-7-yl propionate (**17a**)

Yield: 54%, m.p. = 196.1°C. ^{1}H NMR (600 MHz, Chloroform-*d*), δ (ppm): 7.43 - 7.37 (m, 4H), 7.33 - 7.21 (m, 3H), 7.14 (d, *J* = 2.2 Hz, 1H), 7.08 (dd, *J* = 8.5, 2.2 Hz, 1H), 6.88 (s, 1H), 6.53 (d, *J* = 7.5 Hz, 1H), 5.27 (s, 2H), 4.86 (d, *J* = 1.6 Hz, 2H), 2.63 (q, *J* = 7.5 Hz, 2H), 2.05 (s, 3H), 1.27 (t, *J* = 7.5 Hz, 3H). ^{13}C NMR (125 MHz, Chloroform-*d*), δ (ppm): 173.68, 172.26, 159.52, 153.80, 153.78, 146.28, 141.10, 139.04, 138.11, 137.39, 129.34, 129.03, 128.41, 128.28, 123.12, 119.14, 118.01, 116.05, 110.40, 73.12, 52.43, 27.84, 12.64, 9.00. HRMS m/z: calc. for $C_{26}H_{24}NO_6$ $[M+H]^+$, 446.1598, found 446.1590.

4.5.8. 3-((3-(Benzyloxy)-2-ethyl-4-oxopyridin-1(4*H*)-yl)methyl)-2-oxo-2*H*-chromen-7-yl propionate (**17b**)

Yield: 47%, m.p. = 199.3°C. ^{1}H NMR (600 MHz, Chloroform-*d*), δ (ppm): 7.45 - 7.41 (m, 2H), 7.39 (d, *J* = 8.5 Hz, 1H), 7.31 (dd, *J* = 8.1, 6.6 Hz, 2H), 7.29 - 7.26 (m, 2H), 7.14 (d, *J* = 2.2 Hz, 1H), 7.07 (dd, *J* = 8.5, 2.2 Hz, 1H), 6.83 (s, 1H), 6.53 (d, *J* =

7.5 Hz, 1H), 5.34 (s, 2H), 4.89 (d, *J* = 1.7 Hz, 2H), 2.63 (q, *J* = 7.5 Hz, 2H), 2.50 (q, *J* = 7.5 Hz, 2H), 1.27 (t, *J* = 7.5 Hz, 3H), 1.02 (t, *J* = 7.5 Hz, 3H). ^{13}C NMR (150 MHz, $CDCl_3$), δ (ppm): 173.94, 172.27, 159.52, 153.74, 146.02, 145.90, 139.25, 139.06, 139.02, 137.92, 137.61, 129.04, 128.43, 128.20, 123.71, 119.15, 118.26, 116.04, 110.39, 72.93, 51.86, 27.84, 19.94, 13.56, 9.00. HRMS m/z: calc. for $C_{27}H_{26}NO_6$ $[M+H]^+$, 460.1755, found 460.1748.

4.5.9. 3-((5-(Benzyloxy)-2-methyl-4-oxopyridin-1(4*H*)-yl)methyl)-2-oxo-2*H*-chromen-7-yl propionate (**17c**)

Yield: 47%, m.p. = 104.9°C. ^{1}H NMR (400 MHz, Chloroform-*d*), δ (ppm): 7.39 (d, *J* = 8.5 Hz, 1H), 7.34 (d, *J* = 6.9 Hz, 2H), 7.22 (t, *J* = 7.4 Hz, 2H), 7.18 - 7.09 (m, 2H), 7.07 (dd, *J* = 8.5, 2.2 Hz, 1H), 7.00 (s, 1H), 6.92 (s, 1H), 6.41 (s, 1H), 5.14 (s, 2H), 4.80 (d, *J* = 1.5 Hz, 2H), 2.63 (q, *J* = 7.5 Hz, 2H), 2.23 (s, 3H), 1.27 (t, *J* = 7.5 Hz, 3H). ^{13}C NMR (100 MHz, $CDCl_3$), δ (ppm): 173.40, 172.23, 159.51, 153.73, 153.67, 147.69, 145.52, 138.45, 136.30, 129.13, 128.49, 128.13, 127.88, 127.33, 122.67, 119.01, 118.41, 115.96, 110.26, 71.48, 51.64, 27.74, 19.02, 8.90. HRMS m/z: calc. for $C_{26}H_{24}NO_6$ $[M+H]^+$, 446.1595, found 446.1593.

4.6.General procedure for the preparation of compounds 18a-c, 19a-c, 20a-c, 21a-c, 22a-c, 23a-c.

K_2CO_3 (415 mg, 3 mmol) was added to the solution of **17a** (445 mg, 1 mmol) in 8 mL 50% acetone-water. The mixture was refluxed for 30 min. subsequently, propargyl bromide or corresponding substituted benzyl bromide (1.5 eq) was added, and then the mixture was refluxed for another 6h. The solvent was removed under reduce pressure to obtain yellow solid residue, which was purified by chromatography on silica gel to obtain the corresponding compounds.

4.6.1. 3-(Benzyloxy)-2-methyl-1-((2-oxo-7-(prop-2-yn-1-yloxy)-2*H*-chromen-3-yl)methyl)pyridin-4(1*H*)-one (**18a**)

Yield: 55%, m.p. = 155.4°C. ^{1}H NMR (600 MHz, Chloroform-*d*), δ (ppm): 7.40 (d, *J* = 1.6 Hz, 1H), 7.39 - 7.36 (m, 2H), 7.35 - 7.33 (m, 1H), 7.31 - 7.26 (m, 1H), 7.25 (d, *J* = 8.9 Hz, 1H), 6.94 (m, 2H), 6.57 (d, *J* = 7.4 Hz, 1H), 5.26 (s, 2H), 4.90 - 4.84 (m, 2H), 4.76 (d, *J* = 2.4 Hz, 2H), 2.58 (t, *J* = 2.4 Hz, 1H), 2.16 (s, 2H), 2.08 (s, 3H). ^{13}C

NMR (150 MHz, $CDCl_3$), δ (ppm): 173.37, 161.09, 160.10, 154.90, 146.18, 141.47, 139.14, 139.00, 137.39, 129.32, 128.42, 128.27, 120.41, 117.78, 113.75, 112.66, 102.16, 77.25, 76.90, 73.20, 56.43, 52.53, 31.06, 12.70. HRMS m/z: calc. for $C_{26}H_{22}NO_5$ $[M+H]^+$, 428.1492, found 428.1484.

4.6.2. 3-(Benzyloxy)-2-ethyl-1-((2-oxo-7-(prop-2-yn-1-yloxy)-2*H*-chromen-3-yl)methyl)pyridin-4(1*H*)-one (**18b**)

Yield: 48%, m.p. = 155.4°C. ^{1}H NMR (600 MHz, Chloroform-*d*), δ (ppm): 7.45 (d, *J* = 1.7 Hz, 1H), 7.44 (d, *J* = 1.1 Hz, 1H), 7.35 - 7.24 (m, 6H), 6.96 (d, *J* = 2.1 Hz, 1H), 6.85 (s, 1H), 6.58 (d, *J* = 7.5 Hz, 1H), 5.35 (s, 2H), 4.89 (s, 2H), 4.77 (d, *J* = 2.4 Hz, 2H), 2.58 (t, *J* = 2.4 Hz, 1H), 2.53 (q, *J* = 7.6 Hz, 2H), 1.03 (t, *J* = 7.5 Hz, 3H). ^{13}C NMR (100 MHz, DMSO), δ (ppm): 169.18, 156.15, 155.22, 149.92, 141.19, 141.03, 134.22, 133.60, 132.83, 124.48, 124.16, 123.57, 123.31, 116.29, 113.37, 108.83, 107.81, 97.27, 72.42, 72.06, 68.04, 51.56, 46.96, 15.05, 8.70. HRMS m/z: calc. for $C_{27}H_{24}NO_5$ $[M+H]^+$, 442.1654, found 442.1650.

4.6.3. 5-(Benzyloxy)-2-methyl-1-((2-oxo-7-(prop-2-yn-1-yloxy)-2*H*-chromen-3-yl)methyl)pyridin-4(1*H*)-one (**18c**)

Yield: 46%, m.p. = 121.2°C. ^{1}H NMR (600 MHz, Chloroform-*d*), δ (ppm): 7.36 (d, *J* = 1.5 Hz, 1H), 7.35 (d, 1H), 7.30 (d, *J* = 9.3 Hz, 1H), 7.25 - 7.21 (m, 2H), 7.17 - 7.13 (m, 1H), 6.96 - 6.92 (m, 3H), 6.86 (s, 1H), 6.39 - 6.37 (m, 1H), 5.16 (s, 2H), 4.77 (d, *J* = 2.4 Hz, 2H), 4.75 (d, *J* = 1.5 Hz, 2H), 2.58 (t, *J* = 2.4 Hz, 1H), 2.23 (s, 3H). ^{13}C NMR (100 MHz, $CDCl_3$), δ (ppm): 173.35, 160.98, 160.05, 154.81, 147.61, 145.48, 139.00, 136.44, 129.37, 128.48, 128.08, 127.94, 127.69, 120.10, 118.51, 113.59, 112.53, 102.01, 77.15, 76.80, 71.61, 56.32, 51.64, 19.04. HRMS m/z: calc. for $C_{26}H_{22}NO_5$ $[M+H]^+$, 428.1492, found 428.1486.

4.6.4. 3-(Benzyloxy)-1-((7-(benzyloxy)-2-oxo-2*H*-chromen-3-yl)methyl)-2-methylpyridin-4(1*H*)-one (**19a**)

Yield: 70%, yellow oil. ^{1}H NMR (500 MHz, Chloroform-*d*), δ (ppm): 7.43 - 7.35 (m, 7H), 7.35 - 7.26 (m, 3H), 7.26 - 7.20 (m, 3H), 6.93 (dd, *J* = 8.7, 2.4 Hz, 1H), 6.84 (d, *J* = 2.4 Hz, 1H), 6.46 (d, *J* = 7.5 Hz, 1H), 5.23 (s, 2H), 5.10 (s, 2H), 4.79 (d, *J* = 1.5 Hz, 2H), 2.03 (s, 3H). ^{13}C NMR (150 MHz, $CDCl_3$), δ (ppm): 173.54, 162.14,

159.99, 154.85, 146.08, 140.93, 139.07, 138.80, 137.34, 135.52, 129.19, 129.07, 128.71, 128.38, 128.19, 128.01, 127.43, 119.91, 117.63, 113.62, 112.11, 101.68, 72.87, 70.54, 52.17, 12.42. HRMS m/z: calc. for $C_{30}H_{26}NO_5$ $[M+H]^+$, 480.1805, found 480.1808.

4.6.5. 3-(Benzyloxy)-1-((7-(benzyloxy)-2-oxo-2*H*-chromen-3-yl)methyl)-2-ethylpyridin-4(1*H*)-one (**19b**)

Yield: 37%, yellow oil. ^{1}H NMR (600 MHz, Chloroform-*d*), δ (ppm): 7.45 (d, *J* = 1.6 Hz, 1H), 7.44 (s, 1H), 7.44 - 7.40 (m, 3H), 7.40 (d, *J* = 0.9 Hz, 1H), 7.41 - 7.25 (m, 6H), 6.95 (dd, *J* = 8.7, 2.4 Hz, 1H), 6.89 (d, *J* = 2.4 Hz, 1H), 6.82 (s, 1H), 6.55 (d, *J* = 7.4 Hz, 1H), 5.35 (s, 2H), 5.14 (s, 2H), 4.89 - 4.85 (m, 2H), 2.52 (q, *J* = 7.5 Hz, 2H), 1.03 (t, *J* = 7.5 Hz, 3H). ^{13}C NMR (150 MHz, $CDCl_3$), δ (ppm): 173.86, 162.40, 160.21, 155.02, 146.04, 139.03, 138.69, 137.70, 135.63, 129.33, 129.04, 128.93, 128.84, 128.62, 128.44, 128.18, 127.62, 120.60, 118.18, 113.92, 112.21, 101.94, 72.99, 70.77, 51.90, 19.95, 13.55. HRMS m/z: calc. for $C_{31}H_{28}NO_5$ $[M+H]^+$, 494.1962, found 494.1951.

4.6.6. 5-(Benzyloxy)-1-((7-(benzyloxy)-2-oxo-2*H*-chromen-3-yl)methyl)-2-methylpyridin-4(1*H*)-one (**19c**)

Yield: 40%, yellow oil. ^{1}H NMR (600 MHz, Chloroform-*d*), δ (ppm): 7.44 - 7.27 (m, 9H), 7.22 (t, *J* = 7.7 Hz, 2H), 7.03 (s, 1H), 6.97 - 6.92 (m, 2H), 6.88 (d, *J* = 2.4 Hz, 1H), 6.42 (s, 1H), 5.17 (s, 2H), 5.14 (s, 2H), 4.78 (s, 2H), 2.25 (s, 3H). ^{13}C NMR (150 MHz, $CDCl_3$), δ (ppm): 173.11, 162.42, 160.29, 155.13, 147.59, 145.71, 139.53, 136.50, 135.61, 129.49, 128.92, 128.61, 128.56, 128.17, 128.03, 127.91, 127.60, 119.61, 118.45, 113.87, 112.19, 101.88, 71.73, 70.75, 51.81, 19.17. HRMS m/z: calc. for $C_{30}H_{26}NO_5$ $[M+H]^+$, 480.1805, found 480.1804.

4.6.7. 3-(Benzyloxy)-1-((7-((3-chlorobenzyl)oxy)-2-oxo-2*H*-chromen-3-yl)methyl)-2-methylpyridin-4(1*H*)-one (**20a**)

Yield: 38%, yellow oil. ^{1}H NMR (600 MHz, Chloroform-*d*), δ (ppm): 7.42 (d, *J* = 2.1 Hz, 1H), 7.40 (d, *J* = 1.7 Hz, 1H), 7.39 - 7.38 (m, 1H), 7.37 - 7.22 (m, 8H), 6.94 (dd, *J* = 8.7, 2.4 Hz, 1H), 6.91 (s, 1H), 6.86 (d, *J* = 2.4 Hz, 1H), 6.54 (d, *J* = 7.4 Hz, 1H), 5.26 (s, 2H), 5.10 (s, 2H), 4.85 (s, 2H), 2.07 (s, 3H). ^{13}C NMR (150 MHz,

$CDCl_3$), δ (ppm): 173.41, 162.00, 160.13, 155.02, 146.16, 141.44, 139.15, 139.01, 137.67, 137.37, 134.86, 130.20, 129.45, 129.31, 128.71, 128.40, 128.25, 127.52, 125.48, 120.15, 117.77, 113.78, 112.40, 101.88, 73.18, 69.80, 52.49, 12.69. HRMS m/z: calc. for $C_{30}H_{25}ClNO_5$ $[M+H]^+$, 514.1416, found 514.1423.

4.6.8. 3-(Benzyloxy)-1-((7-((3-chlorobenzyl)oxy)-2-oxo-2*H*-chromen-3-yl)methyl)-2-ethylpyridin-4(1*H*)-one (**20b**)

Yield: 43%, yellow oil. ^{1}H NMR (600 MHz, Chloroform-*d*), δ (ppm): 7.45 (d, 1H), 7.44 (d, *J* = 1.8 Hz, 1H), 7.37 (td, *J* = 8.0, 5.8 Hz, 1H), 7.34 - 7.25 (m, 5H), 7.20 - 7.17 (m, 1H), 7.13 (dt, *J* = 9.5, 2.1 Hz, 1H), 7.04 (td, *J* = 8.5, 2.9 Hz, 1H), 6.94 (dd, *J* = 8.7, 2.4 Hz, 1H), 6.87 (d, *J* = 2.4 Hz, 1H), 6.83 (d, *J* = 2.4 Hz, 1H), 6.54 (d, *J* = 7.3 Hz, 1H), 5.34 (s, 2H), 5.13 (s, 2H), 4.87 (s, 2H), 2.52 (q, *J* = 7.4 Hz, 2H), 1.03 (t, *J* = 7.5 Hz, 3H). ^{13}C NMR (150 MHz, $CDCl_3$), δ (ppm): 173.78, 163.84, 161.91, 160.01, 154.86, 145.89, 138.91, 138.49, 138.11, 137.58, 130.45, 130.39, 129.30, 128.91, 128.32, 128.06, 122.74, 115.44, 115.30, 114.32, 114.17, 113.69, 112.28, 101.82, 72.86, 69.74, 51.76, 19.83, 13.43. HRMS m/z: calc. for $C_{31}H_{27}ClNO_5$ $[M+H]^+$, 528.15726, found 528.1587.

4.6.9. 5-(Benzyloxy)-1-((7-((3-chlorobenzyl)oxy)-2-oxo-2*H*-chromen-3-yl)methyl)-2-methylpyridin-4(1*H*)-one (**20c**)

Yield: 42%, yellow oil. ^{1}H NMR (600 MHz, Chloroform-*d*), δ (ppm): 7.43 (d, *J* = 2.1 Hz, 1H), 7.38 - 7.27 (m, 6H), 7.22 (t, *J* = 7.5 Hz, 2H), 7.13 (t, *J* = 7.4 Hz, 1H), 7.06 (s, 1H), 6.99 (s, 1H), 6.95 (dd, *J* = 8.7, 2.4 Hz, 1H), 6.86 (d, *J* = 2.4 Hz, 1H), 6.45 (s, 1H), 5.17 (s, 2H), 5.12 (s, 2H), 4.81 (s, 2H), 2.27 (s, 3H). ^{13}C NMR (150 MHz, $CDCl_3$), δ (ppm): 172.93, 162.06, 160.24, 155.13, 147.55, 145.82, 139.63, 137.68, 136.46, 134.90, 130.22, 129.64, 128.75, 128.58, 128.19, 128.04, 127.98, 127.54, 125.49, 119.81, 118.39, 113.77, 112.41, 101.89, 71.76, 69.83, 51.87, 19.22. HRMS m/z: calc. for $C_{30}H_{25}ClNO_5$ $[M+H]^+$, 514.1416, found 514.1409.

4.6.10. 3-(Benzyloxy)-1-((7-((3-fluorobenzyl)oxy)-2-oxo-2*H*-chromen-3-yl)methyl)-2-methylpyridin-4(1*H*)-one (**21a**)

Yield: 71%, yellow oil. ^{1}H NMR (600 MHz, Chloroform-*d*), δ (ppm): 7.42 - 7.39 (m, 2H), 7.38 - 7.34 (m, 1H), 7.33 - 7.22 (m, 5H), 7.20 - 7.17 (m, 1H), 7.13 (dt, *J* =

9.4, 2.1 Hz, 1H), 7.04 (td, *J* = 8.5, 2.6, 0.9 Hz, 1H), 6.94 (dd, *J* = 8.7, 2.4 Hz, 1H), 6.86 (t, *J* = 2.3 Hz, 2H), 6.51 (d, *J* = 7.5 Hz, 1H), 5.27 (s, 2H), 5.13 (s, 2H), 4.83 (d, *J* = 1.5 Hz, 2H), 2.05 (s, 3H). ^{13}C NMR (150 MHz, $CDCl_3$), δ (ppm): 173.65, 163.12 (d, $^1J_{C-F}$ = 244.5Hz), 162.03, 160.11, 155.01, 146.27, 141.11, 139.02, 138.74, 138.18 (d, $^3J_{C-F}$ = 7.5 Hz), 137.46, 130.54 (d, $^3J_{C-F}$ = 7.5 Hz), 129.39, 129.33, 128.40, 128.23, 122.87 (d, $^4J_{C-F}$ = 3.0Hz), 120.26, 117.95, 115.48 (d, $^2J_{C-F}$ = 22.5Hz), 114.36 (d, $^2J_{C-F}$ = 22.5Hz), 113.81, 112.38, 101.92, 73.11, 69.85, 52.42, 12.64. HRMS m/z: calc. for $C_{30}H_{25}FNO_5$ $[M+H]^+$, 498.1711, found 498.1711.

4.6.11. 3-(Benzyloxy)-2-ethyl-1-((7-((3-fluorobenzyl)oxy)-2-oxo-2*H*-chromen-3-yl)methyl)pyridin-4(1*H*)-one (**21b**)

Yield: 48%, yellow oil. ^{1}H NMR (600 MHz, Chloroform-*d*), δ (ppm): 7.45 (d, 1H), 7.44 (d, *J* = 1.8 Hz, 1H), 7.37 (td, *J* = 8.0, 5.8 Hz, 1H), 7.34 - 7.25 (m, 5H), 7.20 - 7.17 (m, 1H), 7.13 (dt, *J* = 9.5, 2.1 Hz, 1H), 7.04 (td, *J* = 8.5, 2.9 Hz, 1H), 6.94 (dd, *J* = 8.7, 2.4 Hz, 1H), 6.87 (d, *J* = 2.4 Hz, 1H), 6.83 (d, *J* = 2.4 Hz, 1H), 6.54 (d, *J* = 7.3 Hz, 1H), 5.34 (s, 2H), 5.13 (s, 2H), 4.87 (s, 2H), 2.52 (q, *J* = 7.4 Hz, 2H), 1.03 (t, *J* = 7.5 Hz, 3H). ^{13}C NMR (150 MHz, $CDCl_3$), δ (ppm): 173.78, 163.02(d, $^1J_{C-F}$ = 246.0 Hz), 161.91, 160.01, 154.86, 145.91, 138.91, 138.49, 138.08(d, $^3J_{C-F}$ = 7.5 Hz), 137.58, 130.42(d, $^3J_{C-F}$ = 7.5 Hz), 129.30, 128.92, 128.32, 128.24, 128.06, 122.75(d, $^4J_{C-F}$ = 3.0 Hz), 120.73,118.09, 115.37(d, $^2J_{C-F}$ = 21.0 Hz), 114.24(d, $^2J_{C-F}$ = 22.5 Hz), 113.69, 112.28, 101.82, 72.86, 69.73, 51.76, 19.83, 13.43. HRMS m/z: calc. for $C_{31}H_{27}FNO_5$ $[M+H]^+$, 512.1868, found 512.1845.

4.6.12. 5-(Benzyloxy)-1-((7-((3-fluorobenzyl)oxy)-2-oxo-2*H*-chromen-3-yl)methyl)-2-methylpyridin-4(1*H*)-one (**21c**)

Yield: 38%, yellow oil. ^{1}H NMR (600 MHz, Chloroform-*d*), δ (ppm): 7.39 - 7.33 (m, 3H), 7.31 (d, *J* = 8.6 Hz, 1H), 7.22 (t, *J* = 7.6 Hz, 2H), 7.20 - 7.18 (m, 1H), 7.16 - 7.10 (m, 2H), 7.08 - 7.01 (m, 2H), 6.99 (s, 1H), 6.95 (dd, *J* = 8.7, 2.4 Hz, 1H), 6.86 (d, *J* = 2.4 Hz, 1H), 6.45 (s, 1H), 5.17 (s, 2H), 5.14 (s, 2H), 4.81 (s, 2H), 2.27 (s, 3H). ^{13}C NMR (150 MHz, $CDCl_3$), δ (ppm): 172.86, 163.14(d, $^1J_{C-F}$ = 246.0 Hz), 162.09, 160.24, 155.13, 147.53, 145.83, 139.68, 138.20(d, $^3J_{C-F}$ = 7.5 Hz), 136.46, 130.55(d, $^3J_{C-F}$ = 9.0 Hz), 129.63, 128.57, 128.18, 128.05, 128.02, 122.87(d, $^4J_{C-F}$ = 3.0 Hz),

119.78, 118.38, 115.50(d, $^{2}J_{C\text{-}F}$ = 21.0 Hz), 114.36(d, $^{2}J_{C\text{-}F}$ = 22.5 Hz), 113.79, 112.40, 101.90, 71.77, 69.86, 51.88, 19.21. HRMS m/z: calc. for $C_{30}H_{25}FNO_5$ $[M+H]^+$, 498.1711, found 498.1712.

4.6.13. 3-(Benzyloxy)-1-((7-((4-fluorobenzyl)oxy)-2-oxo-2*H*-chromen-3-yl)methyl)-2-methylpyridin-4(1*H*)-one (**22a**)

Yield: 39%, yellow oil. ^{1}H NMR (600 MHz, Chloroform-*d*), δ (ppm): 7.42 - 7.38 (m, 5H), 7.32 (d, *J* = 8.7 Hz, 1H), 7.30 - 7.23 (m, 3H), 7.11 - 7.06 (m, 2H), 6.94 (dd, *J* = 8.7, 2.4 Hz, 2H), 6.87 (d, *J* = 2.4 Hz, 1H), 6.57 (d, *J* = 7.4 Hz, 1H), 5.26 (s, 2H), 5.09 (s, 2H), 4.86 (s, 2H), 2.08 (s, 3H). ^{13}C NMR (150 MHz, $CDCl_3$), δ (ppm): 173.26, 162.84 (d, $^{1}J_{C\text{-}F}$ = 245.7 Hz), 162.21, 160.19, 155.07, 146.13, 141.65, 139.20, 137.34, 131.39 (d, $^{4}J_{C\text{-}F}$ = 3.3 Hz), 129.58(d, $^{3}J_{C\text{-}F}$ = 8.3 Hz), 129.43, 129.32, 128.45, 128.42, 128.28, 119.98, 117.69, 115.89 (d, $^{2}J_{C\text{-}F}$ = 21.45 Hz), 113.85, 112.29, 101.86, 73.25, 70.06, 52.57, 12.73. HRMS m/z: calc. for $C_{30}H_{25}FNO_5$ $[M+H]^+$, 498.1711, found 498.1708.

4.6.14. 3-(Benzyloxy)-2-ethyl-1-((7-((4-fluorobenzyl)oxy)-2-oxo-2*H*-chromen-3-yl)methyl)pyridin-4(1*H*)-one (**22b**)

Yield: 37%, yellow oil. ^{1}H NMR (600 MHz, Chloroform-*d*), δ (ppm): 7.45 (d, *J* = 1.6 Hz, 1H), 7.44 (d, *J* = 1.3 Hz, 1H), 7.40 (dd, *J* = 8.6, 5.4 Hz, 2H), 7.34 - 7.27 (m, 5H), 7.09 (t, *J* = 8.6 Hz, 2H), 6.93 (dd, *J* = 8.7, 2.4 Hz, 1H), 6.88 (d, *J* = 2.4 Hz, 1H), 6.83 (s, 1H), 6.55 (d, *J* = 7.4 Hz, 1H), 5.35 (s, 2H), 5.09 (s, 2H), 4.87 (s, 2H), 2.52 (q, *J* = 7.5 Hz, 2H), 1.03 (t, *J* = 7.5 Hz, 3H). ^{13}C NMR (150 MHz, $CDCl_3$), δ (ppm): 173.30, 162.74(d, $^{1}J_{C\text{-}F}$ = 246 Hz), 162.07, 160.04, 154.88, 145.94, 138.91, 138.54, 137.57, 131.28(d, $^{4}J_{C\text{-}F}$ = 3.0 Hz), 129.46(d, $^{3}J_{C\text{-}F}$ = 7.5 Hz), 129.47, 129.26, 128.92, 128.33, 128.07, 120.61, 118.06, 115.78(d, $^{2}J_{C\text{-}F}$ = 21.0Hz), 113.73, 112.18, 101.77, 72.88, 69.95, 51.78, 19.83, 13.43. HRMS m/z: calc. for $C_{31}H_{27}FNO_5$ $[M+H]^+$, 512.1868, found 512.1860.

4.6.15. 5-(Benzyloxy)-1-((7-((4-fluorobenzyl)oxy)-2-oxo-2*H*-chromen-3-yl)methyl)-2-methylpyridin-4(1*H*)-one (**22c**)

Yield: 55%, yellow oil. ^{1}H NMR (600 MHz, Chloroform-*d*), δ (ppm): 7.41 (dd, *J* = 8.4, 5.3 Hz, 2H), 7.36 (d, *J* = 7.6 Hz, 2H), 7.31 (d, *J* = 8.6 Hz, 1H), 7.22 (t, *J* = 7.6 Hz,

2H), 7.14 (d, *J* = 7.5 Hz, 1H), 7.09 (t, *J* = 8.6 Hz, 2H), 7.06 (s, 1H), 6.99 (q, *J* = 4.9, 3.7 Hz, 1H), 6.94 (dd, *J* = 8.6, 2.4 Hz, 1H), 6.87 (d, *J* = 2.4 Hz, 1H), 6.44 (s, 1H), 5.17 (s, 2H), 5.10 (s, 2H), 4.80 (s, 2H), 2.27 (s, 3H). ^{13}C NMR (150 MHz, $CDCl_3$), δ (ppm): 172.96, 163.85(d, $^{1}J_{C-F}$ = 244.5 Hz), 162.24, 160.27, 155.15, 147.55, 145.86, 139.69, 136.45, 131.40(d, $^{4}J_{C-F}$ = 3.0 Hz), 129.59, 129.58(d, $^{3}J_{C-F}$ = 9.0 Hz), 128.57, 128.18, 128.04, 127.97, 119.66, 118.36, 115.90(d, $^{2}J_{C-F}$ = 21.0 Hz), 113.81, 112.30, 101.84, 71.76, 70.07, 51.88, 19.22. HRMS m/z: calc. for $C_{30}H_{25}FNO_5$ $[M+H]^+$, 498.1711, found 498.1708.

4.6.16. 3-(Benzyloxy)-1-((7-((3,5-difluorobenzyl)oxy)-2-oxo-2*H*-chromen-3-yl)methyl)-2-methylpyridin-4(1*H*)-one (**23a**)

Yield: 69%, yellow oil. ^{1}H NMR (600 MHz, Chloroform-*d*), δ (ppm): 7.40 (d, *J* = 1.6 Hz, 1H), 7.39 (d, *J* = 1.2 Hz, 1H), 7.33 (d, *J* = 8.7 Hz, 1H), 7.31 (d, *J* = 7.7 Hz, 1H), 7.30 - 7.27 (m, 2H), 7.26 - 7.23 (m, 1H), 6.94 (ddd, *J* = 8.7, 3.9, 2.1 Hz, 3H), 6.88 (s, 1H), 6.85 (d, *J* = 2.4 Hz, 1H), 6.81 - 6.75 (m, 1H), 6.51 (d, *J* = 7.5 Hz, 1H), 5.27 (s, 2H), 5.11 (d, *J* = 2.6 Hz, 2H), 4.83 (d, *J* = 1.5 Hz, 2H), 2.06 (s, 3H). ^{13}C NMR (150 MHz, $CDCl_3$), δ (ppm): 173.67, 163.36 (dd, $^{1}J_{C-F}$ = 247.5, $^{3}J_{C-F}$ = 13.5 Hz), 161.67, 160.04, 154.99, 146.29, 141.10, 139.64(t, $^{3}J_{C-F}$ = 9 Hz), 139.04, 138.71, 137.46, 129.50, 129.32, 128.40, 128.23, 120.48, 117.96, 113.68, 112.58, 109.98(dd, $^{2}J_{C-F}$ = 19.5, $^{3}J_{C-F}$ = 4.5 Hz), 103.88(t, $^{2}J_{C-F}$ = 25.5 Hz), 101.93, 73.11, 69.26, 52.41, 12.65. HRMS m/z: calc. for $C_{30}H_{24}F_2NO_5$ $[M+H]^+$, 516.1617, found 516.1614.

4.6.17. 3-(Benzyloxy)-1-((7-((3,5-difluorobenzyl)oxy)-2-oxo-2*H*-chromen-3-yl)methyl)-2-ethylpyridin-4(1*H*)-one (**23b**)

Yield: 40%, yellow oil. ^{1}H NMR (600 MHz, Chloroform-*d*), δ (ppm): 7.45 (d, *J* = 1.6 Hz, 1H), 7.43 (d, 1H), 7.34 - 7.26 (m, 5H), 6.94 (ddd, *J* = 8.6, 5.5, 2.3 Hz, 3H), 6.85 (d, *J* = 2.4 Hz, 1H), 6.83 (s, 1H), 6.78 (tt, *J* = 8.8, 2.3 Hz, 1H), 6.53 (d, *J* = 7.4 Hz, 1H), 5.34 (s, 2H), 5.11 (s, 2H), 4.87 (s, 2H), 2.52 (q, *J* = 7.5 Hz, 2H), 1.03 (t, *J* = 7.5 Hz, 3H). ^{13}C NMR (150 MHz, $CDCl_3$), δ (ppm): 173.86, 163.37(dd, $^{1}J_{C-F}$ = 249, $^{3}J_{C-F}$ = 13.5 Hz), 161.66, 160.04, 154.94, 146.04, 145.99, 139.65(t, $^{3}J_{C-F}$ = 9.0 Hz), 139.03, 138.53, 137.69, 129.51, 129.02, 128.44, 128.18, 121.07, 118.19, 113.68, 112.59, 109.98(dd, $^{2}J_{C-F}$ = 19.5, $^{3}J_{C-F}$ = 4.5 Hz), 103.88(t, $^{2}J_{C-F}$ = 25.5 Hz), 101.94,

72.97, 69.26, 51.86, 19.94, 13.55. HRMS m/z: calc. for $C_{31}H_{26}F_2NO_5$ $[M+H]^+$, 530.1774, found 530.1753.

4.6.18. 5-(Benzyloxy)-1-((7-((3,5-difluorobenzyl)oxy)-2-oxo-2*H*-chromen-3-yl)methyl)-2-methylpyridin-4(1*H*)-one (**23c**)

Yield: 45%, yellow oil. ^{1}H NMR (600 MHz, Chloroform-*d*), δ (ppm): 7.37 (d, *J* = 1.5 Hz, 1H), 7.36 (s, 1H), 7.33 (d, *J* = 8.7 Hz, 1H), 7.23 (t, *J* = 7.5 Hz, 2H), 7.14 (t, *J* = 7.4 Hz, 1H), 7.06 (s, 1H), 6.99 (s, 1H), 6.95 (ddd, *J* = 8.6, 4.7, 2.3 Hz, 3H), 6.85 (d, *J* = 2.4 Hz, 1H), 6.78 (tt, *J* = 8.8, 2.4 Hz, 1H), 6.44 (s, 1H), 5.18 (s, 2H), 5.12 (s, 2H), 4.81 (s, 2H), 2.26 (s, 3H). ^{13}C NMR (150 MHz, $CDCl_3$), δ (ppm): 172.80, 163.26 (dd, $^1J_{C-F}$ = 247.5, $^3J_{C-F}$ = 13.5 Hz), 161.61, 160.04, 154.98, 147.45, 145.67, 139.5 (t, $^3J_{C-F}$ = 9.0 Hz), 136.36, 129.60, 128.46, 128.06,127.96, 127.94, 127.88, 119.93, 118.30, 113.54, 112.47, 109.87(dd, $^2J_{C-F}$ = 27.0, $^3J_{C-F}$ = 6.0 Hz), 103.78(t, $^2J_{C-F}$ = 25.5Hz), 101.79, 71.65, 69.15, 51.74, 19.09. HRMS m/z: calc. for $C_{30}H_{24}F_2NO_5$ $[M+H]^+$, 516.1617, found 516.1621.

4.7.General procedure for the preparation of compounds 8a-c, 13a-c.

7a was dissolved in anhydrous CH_2Cl_2 (10 mL) and flushed with nitrogen. After the flask was cooled to -48□, boron tribromide (1M in CH_2Cl_2, 1.5eq) was added slowly, and the reaction mixture was allowed to stir at room temperature for 12 h. The reaction mixture was eliminated by the addition of methanol (10 mL) and left to stir for another 0.5 h. The solvent was then evaporated under reduced pressure, and the residues were purified by recrystallization from methanol/ ether to afford the target compound.

4.7.1. 3-Hydroxy-2-methyl-1-((2-oxo-2*H*-chromen-3-yl)methyl)pyridin-4(1*H*)-one hydrobromide (**8a**)

Yield: 90%, m.p. = 269.9□. ^{1}H NMR (600 MHz, DMSO-d_6), δ (ppm): 10.54 (s, 1H), 8.34 (d, *J* = 7.1 Hz, 1H), 7.78 (s, 1H), 7.73 (dd, *J* = 7.8, 1.6 Hz, 1H), 7.65 (ddd, *J* = 8.7, 7.3, 1.6 Hz, 1H), 7.45 (d, *J* = 8.2 Hz, 1H), 7.37 (td, *J* = 7.5, 1.1 Hz, 1H), 7.20 (d, *J* = 7.0 Hz, 1H), 5.47 (d, *J* = 1.3 Hz, 2H), 2.54 (s, 3H). ^{13}C NMR (150 MHz, DMSO), δ (ppm): 159.39, 159.35, 152.91, 143.16, 142.05, 140.89, 139.25, 132.31, 128.77, 124.78, 122.12, 118.54, 116.13, 110.83, 54.83, 12.72. HRMS m/z: calc. for

$C_{16}H_{14}NO_4$ $[M+H]^+$ 284.0917, found 284.0919.

4.7.2. 2-Ethyl-3-hydroxy-1-((2-oxo-2*H*-chromen-3-yl)methyl)pyridin-4(1*H*)-one hydrobromide (**8b**)

Yield: 85%, m.p. = 219.7□. ^{1}H NMR (600 MHz, DMSO-d_6), δ (ppm): 10.60 (s, 1H), 8.29 (d, *J* = 7.0 Hz, 1H), 7.77 (s, 1H), 7.74 (dd, *J* = 7.8, 1.6 Hz, 1H), 7.65 (ddd, *J* = 8.7, 7.4, 1.6 Hz, 1H), 7.47 (d, *J* = 8.3 Hz, 1H), 7.38 (td, *J* = 7.5, 1.0 Hz, 1H), 7.19 (d, *J* = 7.0 Hz, 1H), 5.45 (d, *J* = 1.4 Hz, 2H), 2.95 (q, *J* = 7.4 Hz, 2H), 1.15 (t, *J* = 7.5 Hz, 3H). ^{13}C NMR (150 MHz, DMSO), δ (ppm): 159.67, 159.29, 152.88, 146.11, 143.14, 140.74, 139.05, 132.38, 128.77, 124.87, 122.82, 118.50, 116.17, 111.17, 54.28, 19.88, 11.72. HRMS m/z: calc. for $C_{17}H_{16}NO_4$ $[M+H]^+$ 298.1074, found 298.1073.

4.7.3. 5-Hydroxy-2-methyl-1-((2-oxo-2*H*-chromen-3-yl)methyl)pyridin-4(1*H*)-one hydrobromide (**8c**)

Yield: 73%, m. p. = 257.1□. ^{1}H NMR (600 MHz, DMSO-d_6), δ (ppm): 10.90 (s, 1H), 8.25 (s, 1H), 7.84 (s, 1H), 7.75 (dd, *J* = 7.8, 1.6 Hz, 1H), 7.65 (ddd, *J* = 8.7, 7.3, 1.6 Hz, 1H), 7.46 (d, *J* = 8.2 Hz, 1H), 7.38 (td, *J* = 7.6, 1.1 Hz, 1H), 7.17 (s, 1H), 5.39 (d, 2H), 2.60 (s, 3H). ^{13}C NMR (150 MHz, DMSO), δ (ppm): 161.46, 159.95, 153.43, 149.01, 144.19, 141.61, 132.84, 132.21, 129.29, 125.29, 122.56, 119.01, 116.63, 114.69, 54.73, 19.26. HRMS m/z: calc. for $C_{16}H_{14}NO_4$ $[M+H]^+$ 284.0917, found 284.0911.

4.7.4. 3-Hydroxy-1-((7-methoxy-2-oxo-2*H*-chromen-3-yl)methyl)-2-methylpyridin-4(1*H*)-one hydrobromide (**13a**)

Yield: 43%, m.p. = 253.6□. ^{1}H NMR (600 MHz, DMSO-d_6), δ (ppm): 10.53 (s, 1H), 8.33 (d, *J* = 7.0 Hz, 1H), 7.80 (s, 1H), 7.65 (d, *J* = 8.7 Hz, 1H), 7.19 (d, *J* = 6.9 Hz, 1H), 7.05 (d, *J* = 2.4 Hz, 1H), 6.98 (dd, *J* = 8.7, 2.5 Hz, 1H), 5.42 (d, 2H), 3.86 (s, 3H), 2.54 (s, 3H). ^{13}C NMR (150 MHz, DMSO), δ (ppm): 162.80, 159.79, 159.28, 154.93, 143.10, 141.97, 141.76, 139.18, 129.90, 118.02, 112.76, 112.06, 110.73, 100.53, 56.06, 54.86, 12.74. HRMS m/z: calc. for $C_{17}H_{16}NO_5$ $[M+H]^+$ 314.1023, found 314.1025.

4.7.5. 2-Ethyl-3-hydroxy-1-((7-methoxy-2-oxo-2*H*-chromen-3-yl)methyl)pyridin-4(1*H*)-one hydrobromide (**13b**)

Yield: 61%, m.p. = 214.9□. ^{1}H NMR (500 MHz, Chloroform-*d*), δ (ppm): 10.55 (s,

1H), 8.29 (d, *J* = 7.1, 2.4 Hz, 1H), 7.80 (d, *J* = 2.0 Hz, 1H), 7.66 (d, *J* = 8.8 Hz, 1H), 7.22 - 7.14 (m, 1H), 7.07 (d, *J* = 2.4 Hz, 1H), 6.98 (dd, *J* = 8.7, 2.4 Hz, 1H), 5.41 (s, 2H), 3.86 (s, 3H), 2.96 (q, *J* = 7.5 Hz, 2H), 1.13 (t, *J* = 7.5 Hz, 3H). ^{13}C NMR (100 MHz, DMSO), δ (ppm): 163.36, 160.32, 160.19, 155.42, 146.32, 143.63, 142.21, 139.46, 130.40, 119.16, 113.34, 112.51, 111.55, 101.07, 56.57, 54.75, 20.33, 12.18. HRMS m/z: calc. for $C_{18}H_{18}NO_5$ $[M+H]^+$ 328.1179, found 328.1173.

4.7.6. 5-Hydroxy-2-methyl-1-((2-oxo-2*H*-chromen-3-yl)methyl)pyridin-4(1*H*)-one hydrobromide (**13c**)

Yield: 78%, m.p. = 257.1□. ^{1}H NMR (500 MHz, Chloroform-*d*), δ (ppm): 10.89 (s, 1H), 8.23 (s, 1H), 7.86 (s, 1H), 7.67 (d, *J* = 8.7 Hz, 1H), 7.15 (s, 1H), 7.06 (d, *J* = 2.4 Hz, 1H), 6.98 (dd, *J* = 8.7, 2.4 Hz, 1H), 5.34 (d, 2H), 3.86 (s, 3H), 2.60 (s, 3H). ^{13}C NMR (150 MHz, DMSO), δ (ppm): 162.84, 160.90, 159.87, 154.98, 148.40, 143.63, 142.09, 131.59, 129.93, 117.98, 114.16, 112.80, 112.03, 100.55, 56.07, 54.26, 18.82. HRMS m/z: calc. for $C_{16}H_{14}NO_4$ $[M+H]^+$ 284.0917, found 284.0911.

4.8.General procedure for the preparation of compounds 24a-c, **25a-c**, **26a-c**, **27a-c**, **28a-c**, **29a-c**.

18a was dissolved in anhydrous CH_2Cl_2 (10 mL) and flushed with nitrogen. After the flask was cooled to -48□, boron trichloride (1M in CH_2Cl_2, 1.5eq) was added slowly, and the reaction mixture was allowed to stir at room temperature for 12 h. The reaction mixture was eliminated by the addition of methanol (10 mL) and left to stir for another 0.5 h. The solvent was then evaporated under reduced pressure, and the residues were purified by recrystallization from methanol/ether to afford the target compound.

4.8.1. 3-Hydroxy-2-methyl-1-((2-oxo-7-(prop-2-yn-1-yloxy)-2*H*-chromen-3-yl)methyl)pyridin-4(1*H*)-one hydrochloride (**24a**)

Yield: 77%, m.p. = 228.7□. ^{1}H NMR (600 MHz, DMSO-d_6), δ (ppm): 10.55 (s, 1H), 8.35 (d, *J* = 7.1 Hz, 1H), 7.76 (s, 1H), 7.67 (d, *J* = 8.7 Hz, 1H), 7.44 (d, *J* = 7.0 Hz, 1H), 7.10 (d, *J* = 2.4 Hz, 1H), 7.01 (dd, *J* = 8.7, 2.5 Hz, 1H), 5.46 - 5.38 (m, 2H), 4.94 (d, *J* = 2.4 Hz, 2H), 3.66 (t, *J* = 2.4 Hz, 1H), 2.53 (s, 3H). ^{13}C NMR (150 MHz, DMSO), δ (ppm): 160.44, 159.66, 159.41, 154.58, 143.08, 141.96, 141.36, 139.03,

129.92, 118.62, 113.21, 112.65, 110.78, 101.61, 78.99, 78.42, 56.19, 54.79, 12.72. HRMS m/z calc. for $C_{19}H_{16}NO_5$ $[M+H]^+$ 338.1023, found 338.1012.

4.8.2. 2-Ethyl-3-hydroxy-1-((2-oxo-7-(prop-2-yn-1-yloxy)-2*H*-chromen-3-yl)methyl)pyridin-4(1*H*)-one hydrochloride (**24b**)

Yield: 78%, m.p. = 192.1□. ^{1}H NMR (400 MHz, DMSO-d_6), δ (ppm): 10.57 (s, 1H), 8.31 (d, *J* = 7.0 Hz, 1H), 7.79 (s, 1H), 7.71 (d, *J* = 8.7 Hz, 1H), 7.36 (d, *J* = 6.9 Hz, 1H), 7.14 (d, *J* = 2.5 Hz, 1H), 7.05 (dd, *J* = 8.7, 2.5 Hz, 1H), 5.42 (s, 2H), 4.98 (d, *J* = 2.5 Hz, 2H), 3.69 (t, *J* = 2.4 Hz, 1H), 2.98 (q, *J* = 7.3 Hz, 2H), 1.17 (t, *J* = 7.4 Hz, 3H). ^{13}C NMR (100 MHz, DMSO), δ (ppm): 160.98, 160.41, 160.03, 155.04, 146.26, 143.58, 141.77, 139.32, 130.38, 119.75, 113.75, 113.07, 111.60, 102.13, 79.44, 78.88, 56.67, 54.64, 20.32, 12.16. HRMS m/z calc. for $C_{20}H_{18}NO_5$ $[M+H]^+$ 352.1179, found 352.1191.

4.8.3. 5-Hydroxy-2-methyl-1-((2-oxo-7-(prop-2-yn-1-yloxy)-2*H*-chromen-3-yl)meth yl)pyridin-4(1*H*)-one hydrochloride (**24c**)

Yield: 65%, m.p. = 200.9□. ^{1}H NMR (600 MHz, DMSO-d_6), δ (ppm): 10.90 (s, 1H), 8.26 (s, 1H), 7.79 (s, 1H), 7.69 (d, *J* = 8.7 Hz, 1H), 7.23 (s, 1H), 7.11 (d, *J* = 2.4 Hz, 1H), 7.02 (dd, *J* = 8.7, 2.4 Hz, 1H), 5.31 (s, 2H), 4.95 (d, *J* = 2.4 Hz, 2H), 3.67 (t, *J* = 2.4 Hz, 1H), 2.57 (s, 3H). ^{13}C NMR (100 MHz, DMSO), δ (ppm): 162.18, 160.93, 160.22, 155.09, 148.44, 144.45, 141.90, 131.56, 130.42, 119.27, 114.60, 113.72, 113.11, 102.10, 79.48, 78.91, 56.66, 54.48, 19.25. ESI-MS m/z calc. for $C_{19}H_{16}NO_5$ $[M+H]^+$ 338.1023, found 338.1012.

4.8.4. 1-((7-(Benzyloxy)-2-oxo-2*H*-chromen-3-yl)methyl)-3-hydroxy-2-methylpyridi n-4(1*H*)-one hydrochloride (**25a**)

Yield: 70%, m.p. = 224.4°C. ^{1}H NMR (600 MHz, DMSO-d_6), δ (ppm): 10.52 (s, 1H), 8.32 (d, *J* = 7.1 Hz, 1H), 7.75 (s, 1H), 7.65 (d, *J* = 8.7 Hz, 1H), 7.48 - 7.45 (m, 2H), 7.43 - 7.31 (m, 4H), 7.14 (d, *J* = 2.4 Hz, 1H), 7.04 (dd, *J* = 8.7, 2.4 Hz, 1H), 5.42 - 5.37 (m, 2H), 5.23 (s, 2H), 2.52 (s, 3H). ^{13}C NMR (150 MHz, DMSO), δ (ppm): 161.69, 159.75, 159.60, 154.79, 143.14, 141.66, 141.46, 139.04, 136.17, 129.94, 128.53, 128.13, 127.91, 118.29, 113.37, 112.26, 110.77, 101.45, 69.93, 54.75, 12.69. HRMS m/z: calc. for $C_{23}H_{20}NO_5$ $[M+H]^+$, 390.1336, found 390.1336.

4.8.5. 1-((7-(Benzyloxy)-2-oxo-2*H*-chromen-3-yl)methyl)-2-ethyl-3-hydroxypyridin-4(1*H*)-one hydrochloride (**25b**)

Yield: 64%, m.p. = 214.7°C. ^{1}H NMR (600 MHz, DMSO-d_6), δ (ppm): 10.53 (s, 1H), 8.27 (d, *J* = 7.1 Hz, 1H), 7.75 (s, 1H), 7.66 (d, *J* = 8.7 Hz, 1H), 7.48 - 7.44 (m, 2H), 7.43 - 7.38 (m, 2H), 7.37 - 7.32 (m, 2H), 7.15 (d, *J* = 2.4 Hz, 1H), 7.05 (dd, *J* = 8.7, 2.4 Hz, 1H), 5.39 (s, 2H), 5.23 (s, 2H), 2.95 (q, *J* = 7.4 Hz, 2H), 1.13 (t, *J* = 7.5 Hz, 3H). ^{13}C NMR (150 MHz, DMSO), δ (ppm): 161.75, 159.77, 159.66, 154.77, 145.94, 143.07, 141.42, 138.85, 136.16, 129.94, 128.53, 128.14, 127.93, 118.89, 113.44, 112.22, 111.11, 101.48, 69.96, 54.24, 19.90, 11.71. HRMS m/z: calc. for $C_{24}H_{22}NO_5$ $[M+H]^+$, 404.1492, found 404.1502.

4.8.6. 1-((7-(Benzyloxy)-2-oxo-2*H*-chromen-3-yl)methyl)-5-hydroxy-2-methylpyridin-4(1*H*)-one hydrochloride (**25c**)

Yield: 72%, m.p. = 254.3□. ^{1}H NMR (600 MHz, DMSO-d_6), δ (ppm): 10.85 (s, 1H), 8.25 (s, 1H), 7.80 (s, 1H), 7.68 (d, *J* = 8.7 Hz, 1H), 7.47 (d, *J* = 7.1 Hz, 2H), 7.41 (t, *J* = 7.5 Hz, 2H), 7.38 - 7.33 (m, 1H), 7.22 (s, 1H), 7.15 (d, *J* = 2.3 Hz, 1H), 7.06 (dd, *J* = 8.7, 2.4 Hz, 1H), 5.31 (s, 2H), 5.24 (s, 2H), 2.57 (s, 3H). ^{13}C NMR (150 MHz, DMSO), δ (ppm): 162.21, 162.10, 160.30, 155.31, 148.38, 144.45, 142.17, 136.65, 131.62, 130.45, 129.00, 128.60, 128.38, 118.83, 114.60, 113.87, 112.72, 101.95, 70.43, 54.51, 19.29. HRMS m/z calc. for $C_{23}H_{20}NO_5$ $[M+H]^+$ 390.1336, found 390.1347.

4.8.7. 1-((7-((3-Chlorobenzyl)oxy)-2-oxo-2*H*-chromen-3-yl)methyl)-3-hydroxy-2-methylpyridin-4(1*H*)-one hydrochloride (**26a**)

Yield: 75%, m.p. = 224.4□. ^{1}H NMR (600 MHz, DMSO-d_6), δ (ppm): 10.54 (s, 1H), 8.32 (d, *J* = 7.1 Hz, 1H), 7.74 (s, 1H), 7.66 (d, *J* = 8.7 Hz, 1H), 7.54 (t, *J* = 1.3 Hz, 1H), 7.47 - 7.34 (m, 4H), 7.14 (d, *J* = 2.4 Hz, 1H), 7.05 (dd, *J* = 8.7, 2.4 Hz, 1H), 5.40 (s, 2H), 5.25 (s, 2H), 2.52 (s, 3H). ^{13}C NMR (150 MHz, DMSO), δ (ppm): 161.88, 160.20, 160.08, 155.24, 143.62, 142.16, 141.91, 139.51, 139.25, 133.64, 130.94, 130.47, 128.50, 127.97, 126.85, 118.90, 113.78, 112.90, 111.26, 101.99, 69.40, 55.21, 13.17. HRMS m/z calc. for $C_{23}H_{20}$ NO_5 $[M+H]^+$ 390.1336, found 390.1336.

4.8.8. 1-((7-((3-Chlorobenzyl)oxy)-2-oxo-2*H*-chromen-3-yl)methyl)-2-ethyl-3-hydro

xypyridin-4(1*H*)-one hydrochloride (**26b**)

Yield: 84%, m.p. = 214.7□. ^{1}H NMR (600 MHz, DMSO-d_6), δ (ppm): 10.48 (s, 1H), 8.26 (d, *J* = 7.1 Hz, 1H), 7.74 (s, 1H), 7.67 (d, *J* = 8.7 Hz, 1H), 7.54 (d, *J* = 1.9 Hz, 1H), 7.47 - 7.39 (m, 3H), 7.29 (d, *J* = 7.0 Hz, 1H), 7.15 (d, *J* = 2.5 Hz, 1H), 7.06 (dd, *J* = 8.7, 2.4 Hz, 1H), 5.38 (s, 2H), 5.25 (s, 2H), 2.94 (q, *J* = 7.4 Hz, 2H), 1.13 (t, *J* = 7.5 Hz, 3H). ^{13}C NMR (150 MHz, DMSO), δ (ppm): 161.45, 159.91, 159.63, 154.74, 145.80, 143.10, 141.35, 138.85, 138.77, 133.17, 130.49, 129.99, 128.05, 127.54, 126.41, 119.07, 113.39, 112.38, 111.12, 101.53, 68.95, 54.19, 19.89, 11.72. HRMS m/z calc. for $C_{24}H_{22}NO_5$ $[M+H]^+$ 404.1492, found 404.1502.

4.8.9. 1-((7-((3-Chlorobenzyl)oxy)-2-oxo-2*H*-chromen-3-yl)methyl)-5-hydroxy-2-methylpyridin-4(1*H*)-one hydrochloride (**26c**)

Yield: 64%, m.p. = 254.3□. ^{1}H NMR (600 MHz, DMSO-d_6), δ (ppm): 10.60 (s, 1H), 8.16 (s, 1H), 7.76 (s, 1H), 7.68 (d, *J* = 8.7 Hz, 1H), 7.54 (q, *J* = 1.3 Hz, 1H), 7.46 - 7.39 (m, 3H), 7.15 (d, *J* = 2.4 Hz, 1H), 7.09 (s, 1H), 7.06 (dd, *J* = 8.7, 2.4 Hz, 1H), 5.29 - 5.26 (m, 2H), 5.26 (s, 2H), 2.54 (s, 3H). ^{13}C NMR (100 MHz, DMSO), δ (ppm): 162.68, 161.86, 160.23, 155.22, 148.20, 144.58, 141.94, 139.21, 133.61, 131.06, 130.90, 130.44, 128.46, 127.93, 126.80, 119.06, 114.55, 113.76, 112.84, 101.97, 69.38, 54.27, 19.21. HRMS m/z calc. for $C_{23}H_{20}NO_5$ $[M+H]^+$ 390.1336, found 390.1347.

4.8.10. 1-((7-((3-Fluorobenzyl)oxy)-2-oxo-2*H*-chromen-3-yl)methyl)-3-hydroxy-2-methylpyridin-4(1*H*)-one hydrochloride (**27a**)

Yield: 58%, m.p. = 255.3□. ^{1}H NMR (600 MHz, DMSO-d_6), δ (ppm): 10.52 (s, 1H), 8.32 (d, *J* = 7.1 Hz, 1H), 7.75 (s, 1H), 7.66 (d, *J* = 8.7 Hz, 1H), 7.45 (td, *J* = 7.7, 5.8 Hz, 1H), 7.36 (d, *J* = 7.0 Hz, 1H), 7.33 - 7.28 (m, 2H), 7.21 - 7.15 (m, 1H), 7.14 (d, *J* = 2.5 Hz, 1H), 7.05 (dd, *J* = 8.7, 2.4 Hz, 1H), 5.40 (d, 2H), 5.26 (s, 2H), 2.52 (s, 3H). ^{13}C NMR (150 MHz, DMSO), δ (ppm): 162.17(d, $^{1}J_{C-F}$ = 243 Hz), 161.43, 159.72, 159.56, 154.76, 143.13, 141.72, 141.43, 139.10(d, $^{3}J_{C-F}$ = 7.5 Hz), 139.05, 130.58(d, $^{3}J_{C-F}$ = 7.5 Hz), 129.97, 123.72(d, $^{4}J_{C-F}$ = 3.0 Hz), 118.40, 114.86(d, $^{2}J_{C-F}$ = 19.5 Hz), 114.42(d, $^{2}J_{C-F}$ = 21 Hz), 113.32, 112.39, 110.77, 101.51, 69.00, 54.76, 12.68. HRMS m/z calc. for $C_{23}H_{19}FNO_5$ $[M+H]^+$ 408.1242, found 408.1244.

4.8.11. 2-Ethyl-1-((7-((3-fluorobenzyl)oxy)-2-oxo-2*H*-chromen-3-yl)methyl)-3-hydro

xypyridin-4(1*H*)-one hydrochloride (**27b**)

Yield: 63%, m.p. = 203.4□. ^{1}H NMR (600 MHz, DMSO-d_6), δ (ppm): 10.49 (s, 1H), 8.25 (d, *J* = 7.1 Hz, 1H), 7.74 (s, 1H), 7.67 (d, *J* = 8.7 Hz, 1H), 7.45 (td, *J* = 7.7, 5.7 Hz, 1H), 7.34 - 7.25 (m, 3H), 7.21 - 7.12 (m, 2H), 7.06 (dd, *J* = 8.7, 2.5 Hz, 1H), 5.43 - 5.35 (m, 2H), 5.26 (s, 2H), 2.94 (q, *J* = 7.4 Hz, 2H), 1.13 (t, *J* = 7.5 Hz, 3H). ^{13}C NMR (150 MHz, DMSO), δ (ppm): 162.64(d, $^{1}J_{C-F}$ = 241.5 Hz), 161.94, 160.57, 160.09, 155.20, 143.61, 141.78, 139.56(d, $^{3}J_{C-F}$ = 7.5 Hz), 139.31, 131.06(d, $^{3}J_{C-F}$ = 7.5 Hz), 130.44, 124.22, 124.20, 119.55, 115.35(d, $^{2}J_{C-F}$ = 21 Hz), 114.92(d, $^{2}J_{C-F}$ = 22.5 Hz), 113.85, 112.82, 111.58, 102.01, 69.50, 54.60, 20.31, 12.19. HRMS m/z calc. for $C_{24}H_{21}FNO_5$ $[M+H]^+$ 422.1398, found 422.1408.

4.8.12. 1-((7-((3-Fluorobenzyl)oxy)-2-oxo-2*H*-chromen-3-yl)methyl)-5-hydroxy-2-m ethylpyridin-4(1*H*)-one hydrochloride (**27c**)

Yield: 78%, m. p. = 246.1□. ^{1}H NMR (600 MHz, DMSO-d_6), δ (ppm): 10.52 (s, 1H), 8.12 (s, 1H), 7.74 (s, 1H), 7.68 (d, *J* = 8.7 Hz, 1H), 7.45 (td, *J* = 7.7, 5.9 Hz, 1H), 7.31 (d, *J* = 1.7 Hz, 1H), 7.30 (d, *J* = 2.6 Hz, 1H), 7.20 - 7.15 (m, 1H), 7.14 (d, *J* = 2.4 Hz, 1H), 7.07 - 7.04 (m, 2H), 5.26 (s, 2H), 5.25 (s, 2H), 2.52 (s, 3H). ^{13}C NMR (150 MHz, DMSO), δ (ppm): 163.41, 162.66(d, $^{1}J_{C-F}$ = 241.5 Hz), 161.88, 160.27, 155.23, 148.01, 144.83, 141.79, 139.58(d, $^{3}J_{C-F}$ = 7.5 Hz), 131.06(d, $^{3}J_{C-F}$ = 7.5 Hz), 130.53, 130.45, 124.20(d, $^{4}J_{C-F}$ = 3.0 Hz), 119.25, 115.34(d, $^{2}J_{C-F}$ = 21 Hz), 114.90(d, $^{2}J_{C-F}$ = 22.5 Hz), 114.56, 113.79, 112.87, 101.99, 69.49, 54.11, 19.24. HRMS m/z calc. for $C_{23}H_{19}FNO_5$ $[M+H]^+$ 408.1242, found 408.1237.

4.8.13. 1-((7-((4-Fluorobenzyl)oxy)-2-oxo-2*H*-chromen-3-yl)methyl)-3-hydroxy-2-m ethylpyridin-4(1*H*)-one hydrochloride (**28a**)

Yield: 40%, m.p. = 245□. ^{1}H NMR (600 MHz, DMSO-d_6), δ (ppm): 10.53 (s, 1H), 8.32 (d, *J* = 7.1 Hz, 1H), 7.75 (s, 1H), 7.65 (d, *J* = 8.7 Hz, 1H), 7.54 - 7.51 (m, 2H), 7.36 (d, *J* = 7.1 Hz, 1H), 7.26 - 7.20 (m, 2H), 7.14 (d, *J* = 2.4 Hz, 1H), 7.04 (dd, *J* = 8.7, 2.4 Hz, 1H), 5.40 (s, 2H), 5.21 (s, 2H), 2.52 (s, 3H). ^{13}C NMR (150 MHz, DMSO), δ (ppm): 161.89(d, $^{1}J_{C-F}$ = 243 Hz), 161.57, 159.73, 159.64, 154.78, 143.15, 141.59, 141.44, 139.03, 132.41(d, $^{4}J_{C-F}$ = 3.0 Hz), 130.24(d, $^{3}J_{C-F}$ = 9.0 Hz), 129.93, 118.33, 115.36(d, $^{2}J_{C-F}$ = 21 Hz), 113.34, 112.30, 110.77, 101.46, 69.20, 54.73, 12.68.

HRMS m/z calc. for $C_{23}H_{19}FNO_5$ $[M+H]^+$ 408.1242, found 408.1253.

4.8.14. 2-Ethyl-1-((7-((4-fluorobenzyl)oxy)-2-oxo-2*H*-chromen-3-yl)methyl)-3-hydroxypyridin-4(1*H*)-one hydrochloride (**28b**)

Yield: 42%, m.p. = 179.6□. ^{1}H NMR (600 MHz, DMSO-d_6), δ (ppm): 10.56 (s, 1H), 8.29 (dd, *J* = 7.2, 2.0 Hz, 1H), 7.76 (s, 1H), 7.67 (d, *J* = 8.7 Hz, 1H), 7.56 - 7.51 (m, 2H), 7.39 - 7.33 (m, 1H), 7.27 - 7.22 (m, 2H), 7.16 (d, *J* = 2.4 Hz, 1H), 7.05 (dd, *J* = 8.7, 2.4 Hz, 1H), 5.40 (s, 2H), 5.22 (s, 2H), 2.96 (q, *J* = 7.4 Hz, 2H), 1.14 (t, *J* = 7.5 Hz, 3H). ^{13}C NMR (100 MHz, DMSO), δ (ppm): 162.39(d, $^1J_{C-F}$ = 242 Hz), 162.11, 160.34, 160.12, 155.24, 146.29, 143.57, 141.85, 139.34, 132.88(d, $^4J_{C-F}$ = 3.0 Hz), 130.76(d, $^3J_{C-F}$ = 9.0 Hz), 130.41, 119.43, 115.85(d, $^2J_{C-F}$ = 22 Hz), 113.89, 112.73, 111.58, 101.95, 69.70, 54.68, 20.35, 12.18. ESI-MS m/z calc. for $C_{24}H_{21}FNO_5$ $[M+H]^+$ 422.1398, found 422.1419.

4.8.15. 1-((7-((4-Fluorobenzyl)oxy)-2-oxo-2*H*-chromen-3-yl)methyl)-5-hydroxy-2-methylpyridin-4(1*H*)-one hydrochloride (**28c**)

Yield: 45%, m.p. = 247□. ^{1}H NMR (400 MHz, DMSO-d_6), δ (ppm): 10.87 (s, 1H), 8.26 (s, 1H), 7.80 (s, 1H), 7.67 (d, *J* = 8.7 Hz, 1H), 7.53 (ddd, *J* = 8.6, 5.5, 2.6 Hz, 2H), 7.30 - 7.18 (m, 3H), 7.15 (d, *J* = 2.4 Hz, 1H), 7.05 (dd, *J* = 8.7, 2.4 Hz, 1H), 5.31 (s, 2H), 5.21 (s, 2H), 2.58 (s, 3H). ^{13}C NMR (100 MHz, DMSO), δ (ppm): 161.92(d, $^1J_{C-F}$ = 242 Hz), 161.62, 161.33, 160.71, 159.84, 154.84, 148.08, 143.87, 141.69, 132.42(d, $^4J_{C-F}$ = 3.0 Hz), 130.28(d, $^3J_{C-F}$ = 9.0 Hz), 129.98, 118.36, 115.38(d, $^2J_{C-F}$ = 21 Hz), 114.14, 113.40, 112.28, 101.48, 69.22, 54.14, 18.81. HRMS m/z calc. for $C_{23}H_{19}FNO_5$ $[M+H]^+$ 408.1242, found 408.1243.

4.8.16. 1-((7-((3,5-Difluorobenzyl)oxy)-2-oxo-2*H*-chromen-3-yl)methyl)-3-hydroxy-2-methylpyridin-4(1*H*)-one hydrochloride (**29a**).

Yield: 78%, m.p. = 259.7□. ^{1}H NMR (600 MHz, DMSO-d_6), δ (ppm): 10.51 (s, 1H), 8.32 (d, *J* = 7.0 Hz, 1H), 7.75 (s, 1H), 7.67 (d, *J* = 8.7 Hz, 1H), 7.38 (dd, *J* = 6.9, 2.5 Hz, 1H), 7.24 - 7.18 (m, 3H), 7.14 (d, *J* = 2.4 Hz, 1H), 7.06 (dd, *J* = 8.7, 2.5 Hz, 1H), 5.40 (s, 2H), 5.27 (s, 2H), 2.53 (s, 3H). ^{13}C NMR (150 MHz, DMSO), δ (ppm): 162.88(dd, $^1J_{C-F}$ = 244.5, $^3J_{C-F}$ = 13.5 Hz), 161.63, 160.16, 159.97, 155.20, 143.58, 142.28, 141.87, 141.34(t, $^3J_{C-F}$ = 10.5 Hz), 139.52, 130.49, 118.99, 113.74, 113.00,

111.24, 111.10(dd, $^{2}J_{C\text{-}F}$ = 19.5, $^{4}J_{C\text{-}F}$ = 4.5 Hz), 103.92(t, $^{2}J_{C\text{-}F}$ = 25.5 Hz), 102.03, 68.89, 55.24, 13.17.

HRMS m/z calc. for $C_{23}H_{18}F_2NO_5$ $[M+H]^+$ 426.1148, found 426.1166.

4.8.17. 1-((7-((3,5-Difluorobenzyl)oxy)-2-oxo-2*H*-chromen-3-yl)methyl)-2-ethyl-3-hydroxypyridin-4(1*H*)-one hydrochloride (**29b**)

Yield: 79%, m.p. = 229.0□. ^{1}H NMR (600 MHz, DMSO-d_6), δ (ppm): 10.44 (s, 1H), 8.24 (d, *J* = 7.1 Hz, 1H), 7.73 (s, 1H), 7.68 (d, *J* = 8.7 Hz, 1H), 7.26 (d, *J* = 7.0 Hz, 1H), 7.24 - 7.18 (m, 3H), 7.15 (d, *J* = 2.4 Hz, 1H), 7.07 (dd, *J* = 8.7, 2.4 Hz, 1H), 5.37 (d, 2H), 5.27 (s, 2H), 2.93 (q, *J* = 7.4 Hz, 2H), 1.13 (t, *J* = 7.5 Hz, 3H). ^{13}C NMR (150 MHz, DMSO), δ (ppm): 162.88(dd, $^{1}J_{C\text{-}F}$ = 244.5, $^{3}J_{C\text{-}F}$ = 13.5 Hz), 161.67, 160.71, 160.06, 155.16, 143.64, 142.24, 141.68, 141.32(t, $^{3}J_{C\text{-}F}$ = 9.0 Hz), 139.31, 130.47, 119.72, 113.80, 112.96, 111.59, 111.12(dd, $^{2}J_{C\text{-}F}$ = 19.5, $^{4}J_{C\text{-}F}$ = 4.5 Hz), 103.93(t, $^{2}J_{C\text{-}F}$ = 25.5 Hz), 102.05, 68.91, 54.55, 20.30, 12.20. HRMS m/z calc. for $C_{24}H_{21}FNO_5$ $[M+H]^+$ 422.1398, found 422.1408.

4.8.18. 1-((7-((3,5-Difluorobenzyl)oxy)-2-oxo-2*H*-chromen-3-yl)methyl)-5-hydroxy-2-methylpyridin-4(1*H*)-one hydrochloride (**29c**)

Yield: 85%, m.p. = 237.3□. ^{1}H NMR (600 MHz, DMSO-d_6), δ (ppm): 10.90 (s, 1H), 8.27 (s, 1H), 7.80 (s, 1H), 7.68 (d, *J* = 8.7 Hz, 1H), 7.25 (s, 1H), 7.25 - 7.16 (m, 3H), 7.14 (d, *J* = 2.4 Hz, 1H), 7.07 (dd, *J* = 8.7, 2.4 Hz, 1H), 5.32 (s, 2H), 5.27 (s, 2H), 2.57 (s, 3H). ^{13}C NMR (151 MHz, DMSO), δ (ppm): 162.89(dd, $^{1}J_{C\text{-}F}$ = 246, $^{3}J_{C\text{-}F}$ = 13.5 Hz), 161.78, 161.68, 160.25, 155.25, 148.44, 144.37, 142.15, 141.34(t, $^{3}J_{C\text{-}F}$ = 9.0 Hz), 131.91, 130.53, 119.01, 114.59, 113.78, 112.99, 111.10(dd, $^{2}J_{C\text{-}F}$ = 21.0, $^{4}J_{C\text{-}F}$ = 6.0 Hz), 103.91(t, $^{2}J_{C\text{-}F}$ = 25.5 Hz), 102.04, 68.91, 54.60, 19.31. HRMS m/z calc. for $C_{23}H_{18}F_2NO_5$ $[M+H]^+$ 426.1148, found 426.1145.

4.9. Spectrophotometry methods for pKa determination and pFe^{3+}

The titration was performed by an automated spectrophotometry titration system consisting of an automatic titrator, a luminescence 759s UV-Vis spectrophotometer, and a pH Meter (Mettler Toledo InLab Expert PRO/ Mettler Toledo InLab Science). All instruments were interfaced to a computer and controlled by a Visual Basic

program. For the measurements, the temperature of the probe solution was maintained at 25 ± 0.2□ by a TP-3A temperature controller. A cuvette path length of 50 mm was used and mounted on a spectrophotometer. 0.1 M KCl electrolyte was utilized to maintain the ionic strength, and the solution was stirred vigorously during the titration. The E_0 and S of the pH Meter were calibrated by three standard solutions (pH = 4.00, 6.86, 9.18).

For the p*K***a** determination, the cuvette was charged with 45 mL KCl (0.1 M) solution and 40 μL of saturated EDTA solution. The initial pH value of the solution was acidified to 2.0 with hydrochloric acid (1.5 M). Then 20 μL of test compound DMSO solution (30 μM/ L) was added. The pH of the probe solution was increased by 0.1 pH unit by the addition of 0.1 M KOH from the auto burst. When pH readings varied by < 0.001 pH unit over a 3 s period, an incubation period of 1 min was adopted. At the end of the equilibrium period, the spectrum of the solution was recorded. The cycle was repeated automatically until the defined end point pH value was achieved. The pH-dependent UV profile was recorded over the pH range 2.0 - 10.5, and the test results are analyzed by the HypSpec2014 program.

For the determination of LogK_1, the cuvette was charged with 45 mL KCl (0.1 M) solution, and the initial pH value of the solution was acidified to 2.1 with hydrochloric acid (1.5 M). Subsequently, 30 μM DMSO solution of the testing compound and 60 μL acidic solution of $FeCl_3$ (15.0 mM) were added separately, the ratio of compounds to iron ion was kept at 1.1: 1 (n/ n). After the absorbance value is stabilized, the pH of the probe solution was reduced by 0.1 pH unit by the addition a certain amount of HCl solution (4 M) from the auto burst. After the system was equilibrated, the spectral scan was performed once after 20 min. The cycle was repeated automatically until the defined end point pH value was achieved. the pH-dependent UV profile was recorded over the pH range 0.9-2.1, and the test results are analyzed by the HypSpec2014 program.

For the determination of LogK_2 and LogK_3, the cuvette was charged with 45 mL KCl (0.1 M) solution, and the initial pH value of the solution was acidified to 2.1 with hydrochloric acid (1.5 M). Afterward, 30 μM DMSO solution of the testing

compound and 60 μL acidic solution of $FeCl_3$ (15 mM) were added separately, and the ratio of compounds to iron ion was kept at 5:1 (n/ n). After the system was equilibrated, the pH of the probe solution was increased by 0.1 pH unit by the addition of 0.1 M KOH from the auto burst. When pH readings varied by < 0.001 pH unit over a 3 s period, an incubation period of 1 min was adopted. At the end of the equilibrium period, the spectrum of the solution was recorded. The cycle was repeated automatically until the defined end point pH value was achieved. The pH-dependent UV profile was recorded over the pH range 2.0-10.5, and the test results are analyzed by the HypSpec2014 program.

4.10. Calculation of pFe^{3+}

The values of pFe^{3+} were calculated by HySS software according to the pK_{a1}, pK_{a2}, $\log K_1$, $\log K_2$ and $\log K_3$ determined by the above methods. The $iron^{(III)}$ hydrolysis constants were set as follows: FeOH = -2.563, $Fe(OH)_2$ = -6.205, $Fe(OH)_3$ = -15.1, $Fe_2(OH)_2$ = -2.843, $Fe_3(OH)_4$ = -6.059, $Fe(OH)_4$ = -21.883

4.11. Determination of human MAO-B inhibitory activity

Human MAO-B (5 mg/mL) was purchased from Sigma-Aldrich and was prealiquoted and stored at -80□. 200 μL enzymatic reactions were diluted in 2 mL microcentrifuge tubes by potassium phosphate buffer (Assay Buffer，pH 7.4) which have been provided by Sigma-Aldrich Monoamine Oxidase Assay Kit. The final volumes of the reactions were 100 μL containing 45 μL MAO-B (0.0075 mg/mL), 5 μL different concentrations of the testing inhibitors, and 50 μL Master Reaction, p-Tyramine, HRP Enzyme, and Dye Reagent. Stock solutions of the compounds were prepared in DMSO. The reactions were incubated for 15 min at 37℃ in a flat-black bottom 96-well micro test plate in the dark. The results were quantified in a multi-detection microplate fluorescence reader based on the fluorescence generated (excitation, 535 nm; emission, 585 nm). To calculate the IC_{50} values, data were analyzed using GraphPad PRISM 6 using implemented nonlinear regression fit “one-site competition” [47, 48].

4.12. Molecular modeling studies

Docking simulations were performed using the CDOCKER program in the Discovery Studio 4.5 software (version 4.5, BIOVIA, USA). The crystal structure of MAO-B (PDB entry 2V5Z) with co-crystallized ligand (safinamide) and FAD co-factor was selected as the receptor model[43]. FAD co-factor and three highly conserved water molecules in the active site were retained: HOH 1155, 1170, 1351 (MAO-B, A-chain). Any other crystallized water molecules and ligands were deleted from the protein mode. The chain B in the 2V5Z was deleted, and all computations were performed in chain A. All the parameters for the protein preparation, ligands minimization, ligand preparation, and docking run were set to their default values.

4.13. Cytotoxicity and cytoprotection test.

Cell culture: Human glioma U251 were obtained from Zhejiang University (Zhejiang, China). Cells were maintained in a humidified incubator with 5% CO_2 at 37°C in Dulbecco's modified Eagle's medium (DMEM) supplemented with 10% heat-inactivated fetal bovine serum (Solarbio, Beijing, China), 100 units/mL penicillin, and 100 μg/mL of streptomycin (Beyotime, Beijing, China).

Cytotoxicity and cytoprotection test: Human glioma cells were seeded in 96-well plates at the density of 3×10^3 cells/well. The cells were pretreated with **27a** (100 μM) for 24 h and then exposed to 100 μM H_2O_2 or medium for additional 1 h, incubation of the cells was continued for 1 h, then the cell viability was measured by MTS assay according to the manufacturer's instruction (MTS assay kit, Cell Titer 96® Aqueous One Solution, Promega) [44, 45]. For the cytotoxicity test, cells were treated with compounds at concentrations of 10 nM, 10μM, and 100 μM. Data were processed by GraphPad Prism 6. $^{###}p < 0.001$ compared to the control, $*p < 0.05$ compared to H_2O_2-treated cells

4.14. Morris water maze test

Behavioral studies were performed by using adult male ICR mice (8-10 weeks

old, weight 20-25 g) purchased from the Zhejiang Academy of Medical Sciences (Hangzhou, China). Pargyline and Scopolamine hydrobromide were supplied by Aladdin Reagents (N159008, S107418, Shanghai, China). The test agent was prepared as a clear injection, which consists of 10% DMSO, 20% (2-Hydroxypropyl)-β-cyclodextrin and phosphate buffered saline.

The mice were divided into four groups as follows: (i) vehicle as the blank control, (ii) scopolamine as the model group, (iii) compound **27a** plus scopolamine as the test group, (iv) pargyline plus scopolamine as the positive control. For two consecutive weeks, 30 min before the intraperitoneal injection of scopolamine (1 $mg \cdot kg^{-1}$) or blank solution, **27a**, and pargyline (10 $mg \cdot kg^{-1}$) were intraperitoneally injected to mice in groups (iii) and (iv) respectively. Cognitive function was evaluated by the ANY-maze Video Tracking System. In a well-lit room, Morris water maze was placed. The opaque circular pool (120 cm diameter, 60 cm height) was filled with water (40 cm, depth) and sustained at 25□. The maze was divided into four equal quadrants, and an escape platform (10 cm diameter) was located in the center of the fourth quadrant of the maze, which was labeled by a small flag (5 cm tall).

The behavioral study consists of 2 days learning and memory training, the mice were trained to find the platform for one trial of each quadrant, and every quadrant lasted for 120 s. If the mouse reaches the platform (a successful escape) within 120 s, the time would be recorded. If failed, the test was terminated, and the animal will be guided to the platform gently. The mice were kept on the platform for 10 s, no matter if they could find the platform within the stipulated time or not.

For the cognitive evaluation, each mouse was individually evaluated on both visible-platform (days 3-4) and hidden-platform (days 5) versions of the water maze. On the last day (day 5), the platform was removed and the animals were given a probe trial in which they had 120 s to search for the platform. The time of escape latency and the number of times that animals crossed the platform location and the number of times that animals enter the target quadrant were recorded. All the data were recorded by ANY-maze Video Tracking System and processed by GraphPad Prism 6 [46].

Acknowledgments

This project was supported by the National Natural Science Foundation of China, NSFC (Grant No. 21576239 and 81803340). We would like to thank Meng Yu from the Institute of medicinal plant development (IMPLAD) for his help in the docking study.

Reference

[1] Alzheimer's Association, 2019 Alzheimer's disease facts and figures, Alzheimer's Dementia. 15 (2019) 321-387.
[2] M.G. Savelieff, S. Lee, Y.Z. Liu, M.H. Lim, Untangling Amyloid-beta, Tau, and Metals in Alzheimer's Disease, Acs Chem. Biol., 8 (2013) 856-865.
[3] Z. Chen, M. Digiacomo, Y. Tu, Q. Gu, S. Wang, X. Yang, J. Chu, Q. Chen, Y. Han, J. Chen, G. Nesi, S. Sestito, M. Macchia, S. Rapposelli, R. Pi, Discovery of novel rivastigmine-hydroxycinnamic acid hybrids as multi-targeted agents for Alzheimer's disease, Eur. J. Med. Chem. 125 (2017) 784-792.
[4] J. Wang, P. Cai, X.L. Yang, F. Li, J.J. Wu, L.Y. Kong, X.B. Wang, Novel cinnamamide-dibenzylamine hybrids: Potent neurogenic agents with antioxidant, cholinergic, and neuroprotective properties as innovative drugs for Alzheimer's disease, Eur. J. Med. Chem. 139 (2017) 68-83.
[5] M.G. Savelieff, G. Nam, J. Kang, H.J. Lee, M. Lee, M.H. Lim, Development of multifunctional molecules as potential therapeutic candidates for Alzheimer's Disease, Parkinson's Disease, and Amyotrophic Lateral Sclerosis in the last decade, Chem Rev. 119 (2018) 1221-1322.
[6] J. Hroudova, N. Singh, Z. Fisar, K.K. Ghosh, Progress in drug development for Alzheimer's disease: An overview in relation to mitochondria energy metabolism, Eur. J. Med. Chem. 121 (2016) 774-784.
[7] J.P.M. Finberg, J.M. Rabey, Inhibitors of MAO-A and MAO-B in psychiatry and neurology, Front. Pharmacol. 7 (2016) 340-354.
[8] M.B.H. Youdim, D. Edmondson, K.F. Tipton, The therapeutic potential of monoamine oxidase inhibitors, Nat. Rev. Neurosci. 7 (2006) 295-309.
[9] K.N. Westlund, R.M. Denney, L.M. Kochersperger, R.M. Rose, C.W. Abell, Distinct monoamine oxidase A and B populations in primate brain, Science 230 (1985) 181-183.
[10] E.D. Deeks, Safinamide: First Global Approval, Drugs 75 (2015) 705-711.
[11] S. Carradori, R. Silvestri, New frontiers in selective human MAO-B inhibitors, J. Med. Chem. 58 (2015) 6717-6732.
[12] C.A. Cobb, M.P. Cole, Oxidative and nitrative stress in neurodegeneration, Neurobiol. Dis. 84 (2015) 4-21.
[13] J.C. Shih, K. Chen, M.J. Ridd, Monoamine oxidase: From genes to behavior, Annu. Rev. Neurosci. 22 (1999) 197-217.
[14] J.H. Park, Y.H. Ju, J.W. Choi, H.J. Song, B.K. Jang, J. Woo, H. Chun, H.J. Kim,

S.J. Shin, O. Yarishkin, S. Jo, M. Park, S.K. Yeon, S. Kim, J. Kim, M.H. Nam, A.M. Londhe, J. Kim, S.J. Cho, S. Cho, C. Lee, S.Y. Hwang, S.W. Kim, S.J. Oh, J. Cho, A.N. Pae, C.J. Lee, K.D. Park, Newly developed reversible MAO-B inhibitor circumvents the shortcomings of irreversible inhibitors in Alzheimer's disease, Sci. Adv. 5 (2019).

[15] R.C. Hider, X. Kong, Iron speciation in the cytosol: an overview, Dalton Trans. 42 (2013) 3220-3229.

[16] O. Weinreb, S. Mandel, O. Bar-Am, T. Amit, Iron-chelating backbone coupled with monoamine oxidase inhibitory moiety as novel pluripotential therapeutic agents for Alzheimer's disease: a tribute to Moussa Youdim, J. Neural. Transm. 118 (2011) 479-492.

[17] R.C. Hider, S. Roy, Y.M. Ma, X. Le Kong, J. Preston, The potential application of iron chelators for the treatment of neurodegenerative diseases, Metallomics, 3 (2011) 239-249.

[18] M. Huang, S.S. Xie, N. Jiang, J.S. Lan, L.Y. Kong, X.B. Wang, Multifunctional coumarin derivatives: Monoamine oxidase B (MAO-B) inhibition, anti-β-amyloid (Aβ) aggregation and metal chelation properties against Alzheimer’s disease, Bioorg. Med. Chem. Lett. 25 (2015) 508-513.

[19] M. Schrag, C. Mueller, M. Zabel, A. Crofton, W.M. Kirsch, O. Ghribi, R. Squitti, G. Perry, Oxidative stress in blood in Alzheimer's disease and mild cognitive impairment: A meta-analysis, Neurobiol. Dis. 59 (2013) 100-110.

[20] E. Gumienna-Kontecka, M. Pyrkosz-Bulska, A. Szebesczyk, M. Ostrowska, Iron chelating strategies in systemic metal overload, neurodegeneration and cancer, Curr. Med. Chem. 21 (2014) 3741-3767.

[21] S. Rivera-Mancía, I. Pérez-Neri, C. Ríos, L. Tristán-López, L. Rivera-Espinosa, S. Montes, The transition metals copper and iron in neurodegenerative diseases, Chem-Biol. Interact. 186 (2010) 184-199.

[22] N. Guzior, A. Wieckowska, D. Panek, B. Malawska, Recent development of multifunctional agents as potential drug candidates for the treatment of Alzheimerμs Disease, Curr. Med. Chem., 22 (2015) 373-404.

[23] M.A. Santos, K. Chand, S. Chaves, Recent progress in multifunctional metal chelators as potential drugs for Alzheimer's disease, Coordin. Chem. Rev. 327–328 (2016) 287-303.

[24] L. Wang, G. Esteban, M. Ojima, O.M. Bautista-Aguilera, T. Inokuchi, I. Moraleda, I. Iriepa, A. Samadi, M.B. Youdim, A. Romero, E. Soriano, R. Herrero, A.P. Fernandez Fernandez, M. Ricardo Martinez, J. Marco-Contelles, M. Unzeta, Donepezil + propargylamine + 8-hydroxyquinoline hybrids as new multifunctional metal-chelators, ChE and MAO inhibitors for the potential treatment of Alzheimer's disease, Eur. J. Med. Chem. 80 (2014) 543-561.

[25] Zhisheng Mi, Bing Gan, Sihang Yu, Xiaoying Jiang, Changjun Zhang, Tao Zhou, Jing Su, Renren Bai, Y. Xie, Dual-target anti-Alzheimer's disease agents with both iron ion chelating and monoamine oxidase-B inhibitory activity, J. Enzym. Inhib. Med. Chem. (2019), doi: https://doi.org/10.1080/14756366.2019.1634703.

[26] A.C. Tripathi, S. Upadhyay, S. Paliwal, S.K. Saraf, Privileged scaffolds as MAO

inhibitors: Retrospect and prospects, Eur. J. Med. Chem. 145 (2018) 445-497.
[27] C. Gnerre, M. Catto, F. Leonetti, P. Weber, P.-A. Carrupt, C. Altomare, A. Carotti, B. Testa, Inhibition of monoamine oxidases by functionalized coumarin derivatives: Biological activities, QSARs, and 3D-QSARs, J. Med. Chem, 43 (2000) 4747-4758..
[28] C. Bruhlmann, F. Ooms, P.A. Carrupt, B. Testa, M. Catto, F. Leonetti, C. Altomare, A. Carotti, Coumarins derivatives as dual inhibitors of acetylcholinesterase and monoamine oxidase, J. Med. Chem. 44 (2001) 3195-3198.
[29] L. Santana, H. Gonzalez-Diaz, E. Quezada, E. Uriarte, M. Yanez, D. Vina, F. Orallo, Quantitative structure-activity relationship and complex network approach to monoamine oxidase A and B inhibitors, J. Med. Chem. 51 (2008) 6740-6751.
[30] B. Mathew, S. Dev, M. Joy, G.E. Mathew, A. Marathakam, G.K. Krishnan, Refining the structural features of chromones as selective MAO-B inhibitors: Exploration of combined pharmacophore-based 3D-QSAR and quantum chemical studies, ChemistrySelect. 2 (2017) 11645-11652.
[31] M.J. Matos, D. Vina, E. Quezada, C. Picciau, G. Delogu, F. Orallo, L. Santana, E. Uriarte, A new series of 3-phenylcoumarins as potent and selective MAO-B inhibitors, Bioorg. Med. Chem. Lett. 19 (2009) 3268-3270.
[32] M.J. Matos, D. Vina, C. Picciau, F. Orallo, L. Santana, E. Uriarte, Synthesis and evaluation of 6-methyl-3-phenylcoumarins as potent and selective MAO-B inhibitors, Bioorg. Med. Chem. Lett. 19 (2009) 5053-5055.
[33] G. Delogu, C. Picciau, G. Ferino, E. Quezada, G. Podda, E. Uriarte, D. Vina, Synthesis, human monoamine oxidase inhibitory activity and molecular docking studies of 3-heteroarylcoumarin derivatives, Eur. J. Med. Chem. 46 (2011) 1147-1152.
[34] M.D. Mertens, S. Hinz, C.E. Mueller, M. Guetschow, Alkynyl-coumarinyl ethers as MAO-B inhibitors, Bioorg. Med. Chem. 22 (2014) 1916-1928.
[35] L. Pisani, R.M. Iacobazzi, M. Catto, M. Rullo, R. Farina, N. Denora, S. Cellamare, C.D. Altomare, Investigating alkyl nitrates as nitric oxide releasing precursors of multitarget acetylcholinesterase-monoamine oxidase B inhibitors, Eur. J. Med. Chem. 161 (2019) 292-309.
[36] Y.Y. Xie, Z. Lu, X.L. Kong, T. Zhou, S. Bansal, R. Hider, Systematic comparison of the mono-, dimethyl- and trimethyl 3-hydroxy-4(1*H*)-pyridones - Attempted optimization of the orally active iron chelator, deferiprone, Eur. J. Med. Chem. 115 (2016) 132-140.
[37] A. Fassihi, D. Abedi, L. Saghaie, R. Sabet, H. Fazeli, G. Bostaki, O. Deilami, H. Sadinpour, Synthesis, antimicrobial evaluation and QSAR study of some 3-hydroxypyridine-4-one and 3-hydroxypyran-4-one derivatives, Eur. J. Med. Chem. 44 (2009) 2145-2157.
[38] X.W. Ye, Y.C. Zheng, Y.C. Duan, M.M. Wang, B. Yu, J.L. Ren, J.L. Ma, E. Zhang, H.M. Liu, Synthesis and biological evaluation of coumarin-1,2,3-triazole-dithiocarbamate hybrids as potent LSD1 inhibitors, Med. Chem. Commun. 5 (2014) 650-654.
[39] F. Belluti, G. Fontana, L. Dal Bo, N. Carenini, C. Giommarelli, F. Zunino, Design, synthesis and anticancer activities of stilbene-coumarin hybrid compounds: Identification of novel proapoptotic agents, Bioorg. Med. Chem. 18 (2010)

3543-3550..
[40] Y. Ma, S. Roy, X. Kong, Y. Chen, D. Liu, R.C. Hider, Design and synthesis of fluorinated iron chelators for metabolic study and brain uptake, J. Med. Chem. 55 (2012) 2185-2195.
[41] Y. Ma, X. Kong, Y.L. Chen, R.C. Hider, Synthesis and characterizations of pyridazine-based iron chelators, Dalton Trans. 43 (2014) 17120-17128.
[42] Y.L. Chen, D.J. Barlow, X.L. Kong, Y.M. Ma, R.C. Hider, Prediction of 3-hydroxypyridin-4-one (HPO) log K_1 values for $Fe^{(III)}$, Dalton Trans. 41 (2012) 10784-10791.
[43] C. Binda, J. Wang, L. Pisani, C. Caccia, A. Carotti, P. Salvati, D.E. Edmondson, A. Mattevi, Structures of human monoamine oxidase B complexes with selective noncovalent inhibitors: Safinamide and coumarin analogs, J. Med. Chem. 50 (2007) 5848-5852.
[44] S. Gao, T. Qin, Z. Liu, M.A. Caceres, C.F. Ronchi, C.Y.O. Chen, K.j. Yeum, A. Taylor, J.B. Blumberg, Y. Liu, F. Shang, Lutein and zeaxanthin supplementation reduces H_2O_2-induced oxidative damage in human lens epithelial cells, Mol. Vis. 17 (2011) 3180-3190.
[45] H.L. Yang, P. Cai, Q.H. Liu, X.L. Yang, F. Li, J. Wang, J.J. Wu, X.B. Wang, L.Y. Kong, Design, synthesis and evaluation of coumarin-pargyline hybrids as novel dual inhibitors of monoamine oxidases and amyloid-β aggregation for the treatment of Alzheimer's disease, Eur. J. Med. Chem. 138 (2017) 715-728.
[46] Y. Chen, H. Lin, J. Zhu, K. Gu, Q. Li, S. He, X. Lu, R. Tan, Y. Pei, L. Wu, Y. Bian, H. Sun, Design, synthesis, in vitro and in vivo evaluation of tacrine-cinnamic acid hybrids as multi-target acetyl-and butyrylcholinesterase inhibitors against Alzheimer's disease, Rsc Adv. 7 (2017) 33851-33867.
[47] B. Strydom, J.J. Bergh, J.P. Petzer, 8-Aryl- and alkyloxycaffeine analogues as inhibitors of monoamine oxidase, Eur. J. Med. Chem. 46 (2011) 3474-3485.

Tables, schemes and figures

Table 1. The pK_a and pFe^{3+} values of the synthesized compounds[a]

Compounds	pK_{a1}	pK_{a2}	LogK_1	LogK_2	LogK_3	pFe^{3+}
8a	3.07	9.68	14.67	25.93	34.64	18.36
8b	3.03	9.70	14.46	25.60	34.03	17.72
8c	3.14	8.97	13.75	24.38	32.82	18.62
13a	3.13	9.66	14.64	25.88	34.54	18.32
13b	3.09	9.70	14.55	25.67	34.26	17.93
13c	3.15	9.00	13.52	24.28	32.26	18.00
24a	3.11	9.58	14.66	25.66	33.86	17.93
24b	2.95	9.63	14.11	25.26	33.91	17.78
24c	3.07	8.94	13.65	24.04	31.75	17.68
25a	3.11	9.61	14.80	25.46	34.74	18.64
25b	3.11	9.71	14.69	25.61	34.46	18.08
25c	3.12	9.03	15.07	23.26	31.23	16.89
26a	3.17	9.67	14.17	24.95	32.82	16.73
26b	3.10	9.76	15.21	25.27	34.53	17.99
26c	3.16	9.07	14.77	24.50	33.25	18.75
27a	3.10	9.65	14.26	25.32	34.25	18.04
27b	3.12	9.69	14.75	25.72	34.65	18.32
27c	3.15	8.99	13.66	24.13	32.71	18.44
28a	3.24	9.51	14.72	25.74	34.47	18.67
28b	3.15	9.62	14.95	25.82	34.27	18.27
28c	3.26	8.87	14.74	24.91	32.50	18.65
29a	3.10	9.54	14.32	23.79	32.71	16.84
29b	3.08	9.70	14.82	25.68	34.83	18.47
29c	3.11	8.95	15.02	24.88	31.67	17.86
Deferiprone	3.65	9.89	15.28	26.31	33.55	17.26

				27.66[b]	37.32[b]	20.39[b]
Deferiprone	3.67[c]	9.78[c]	15.03[c]	27.42[c]	37.35[c]	20.70[c]

[a]The compounds were tested in DMSO: KCl (0.1 M) = 2: 3 (V/ V) to address the solubility issue.

[b]The data were measured in a 0.1 M KCl solution.

[c]The data from reference tested in a 0.1 M KCl solution [36].

Table 2. The MAO-B inhibitory activities of the targeted compounds.

Compound	Inhibitory rate (%,10 μM)	Compound	Inhibitory rate (%,10 μM)
8a	22.4%	**26a**	21.2%
8b	25.0%	**26b**	92.5%
8c	6.8%	**26c**	82.0%
13a	94.4%	**27a**	81.3%
13b	50.7%	**27b**	91.9%
13c	38.3%	**27c**	85.8%
24a	47.1%	**28a**	90.9%
24b	78.1%	**28b**	91.6%
24c	50.6%	**28c**	87.6%
25a	89.6%	**29a**	67.5%
25b	91.9%	**29b**	91.7%
25c	86.5%	**29c**	68.1%

Table 3. The anti-MAO-B IC_{50} values of the selected compounds.

Compound	IC_{50} (nM)	Compound	IC_{50} (nM)
13a	91.9	**27a**	**14.7**
24b	120.9	**27b**	264.9
25a	335.7	**27c**	192.6
25b	128.6	**28a**	301.3
25c	289.9	**28b**	163.1
26b	424.6	**28c**	145.1
26c	126.5	**29b**	223.1
Pargyline	85.8		

Table 4. Effects of **27a** (10 $mg \cdot kg^{-1}$) on scopolamine-induced memory impairment in ICR mice evaluated by the Morris water maze test. Pargyline (10 $mg \cdot kg^{-1}$) was used as the reference drug. Data were presented as the mean ± SEM (n = 8; $^{\#}p < 0.05$, $^{\#\#}p < 0.01$, $^{\#\#\#}p < 0.001$, Control group vs. scopolamine model group; *p < 0.05, **p< 0.01, ***p< 0.001, **27a** or pargyline group vs. scopolamine model group).

Group	Latency to target (s)	Distance to target (m)	Target quadrant times
Control	15.3 ± 1.2	5.8 ± 0.7	16.5 ± 0.8
Model	40.2 ± 10.5$^{\#}$	10.4 ± 1.2$^{\#\#}$	9.0 ± 0.8$^{\#\#\#}$
27a	9.6 ± 3.4*	4.2 ± 0.6***	16.6 ± 1.1***
Pargyline	5.6 ± 2.0*	6.6 ± 0.6*	16.3 ± 1.5***

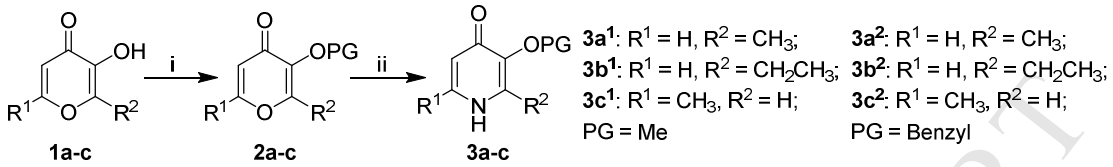

Scheme 1. Reagents and conditions: (i) Iodomethane or benzyl bromide, K_2CO_3, acetone, reflux, 8 h. (ii) 25% NH_4OH, 50% ethanol-H_2O, reflux, 12 h.

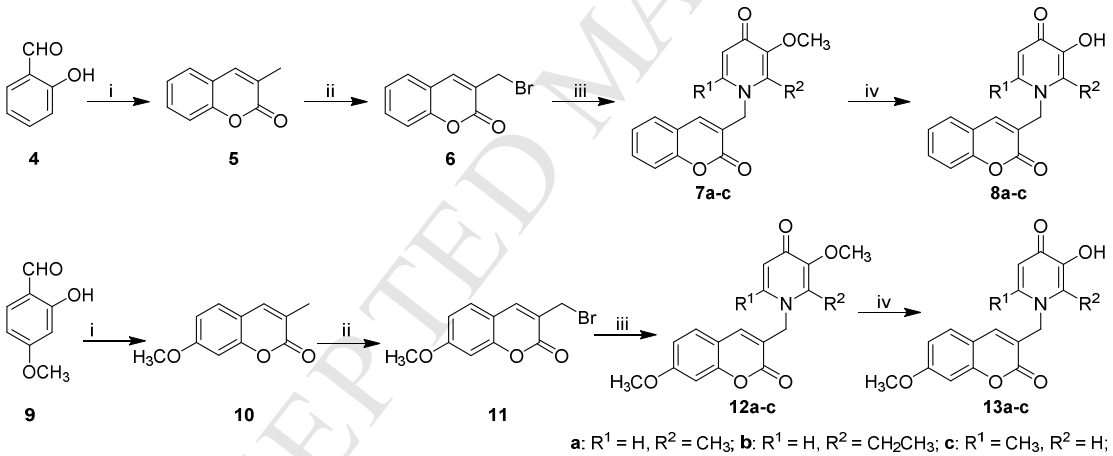

Scheme 2. Reagents and conditions: (i) Propionic anhydride, sodium propionate, triethylamine, 170□, 10 h. (ii) NBS, BPO, CCl_4, reflux, 12 h. (iii) **3a**, **3b**, or **3c**, K_2CO_3, acetonitrile, reflux, 6 h. (iv) BBr_3, DCM anhydrous, - 48□ to r.t., 12 h.

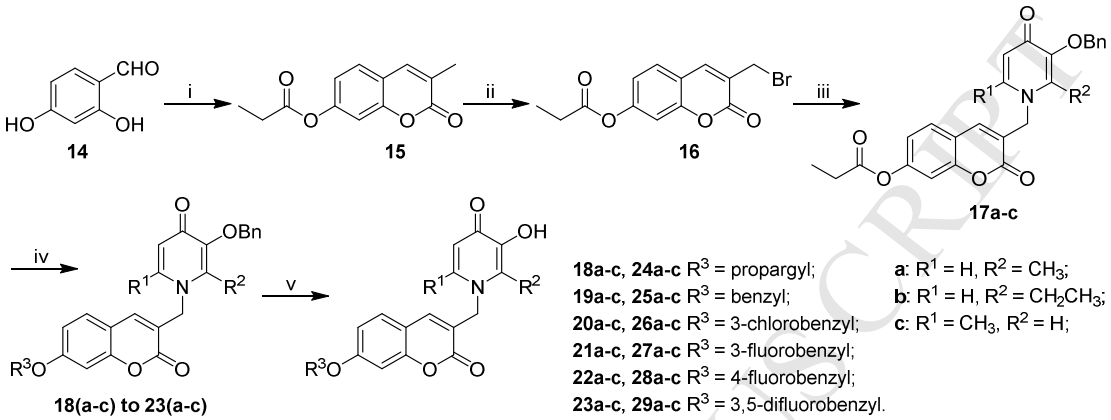

Scheme 3. Reagents and conditions: (i) Propionic anhydride, sodium propionate, triethylamine, 170□, 10 h. (ii) NBS, BPO, CCl_4, reflux, 12 h. (iii) **3a**, **3b**, or **3c**, K_2CO_3, acetonitrile, reflux, 6 h. (iv) Propargyl bromide or corresponding substituted benzyl bromide, K_2CO_3, 50% acetone-H_2O, reflux, 6 h. (v) BCl_3, anhydrous DCM, - 48□ to r.t. 12 h.

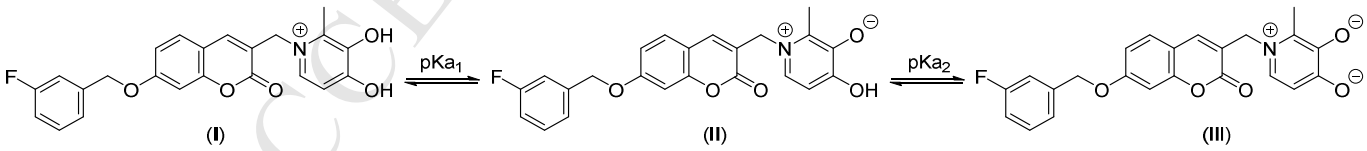

Scheme 4. The ionization of compound **27a**

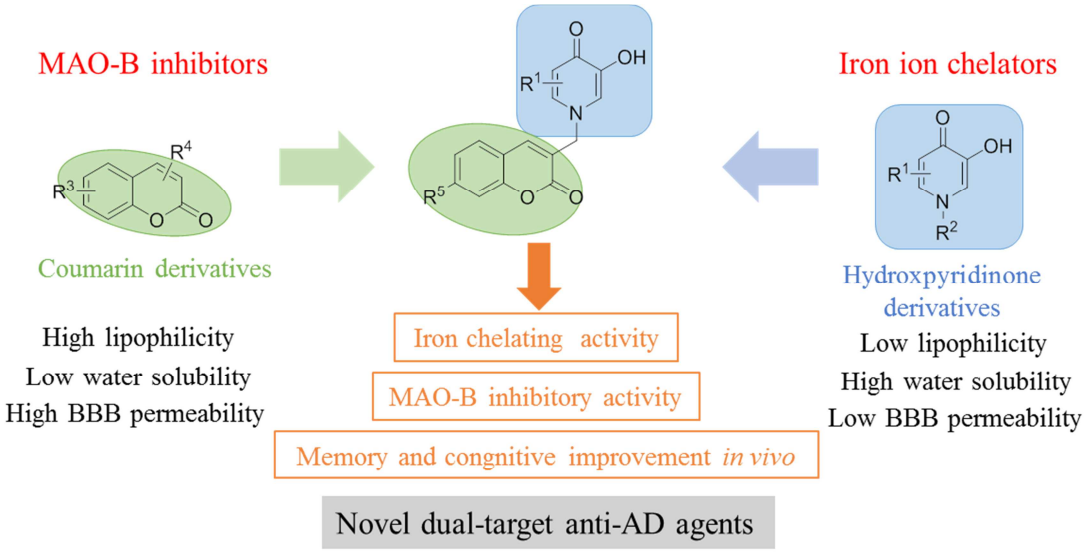

Fig. 1. Strategy for the design of dual-target anti-AD agents.

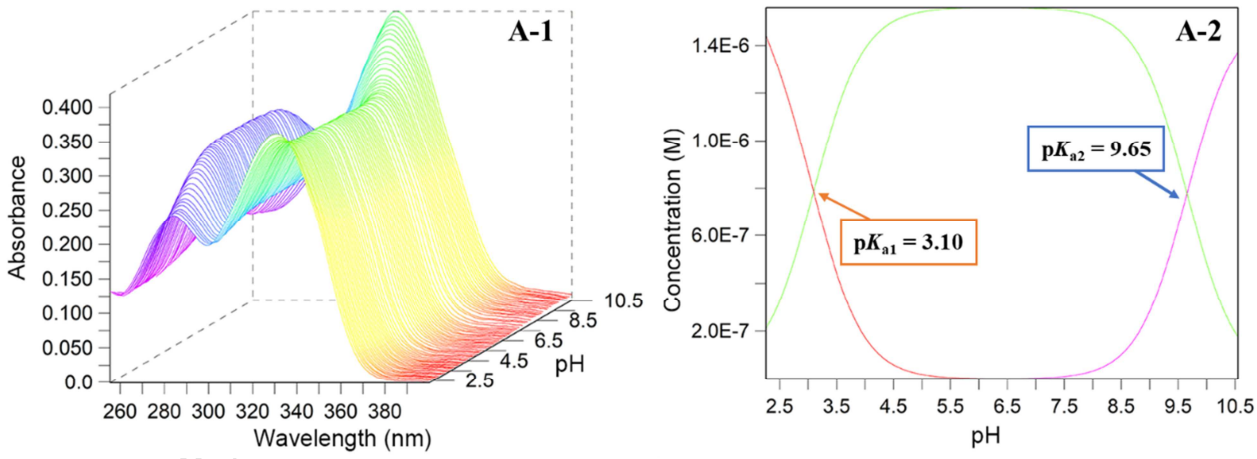

Fig. **2**. The pH-dependent UV spectra of compound **27a. A-1**. The pH-dependence of the titration spectrum of compound **27a**. **A-2**. The pK_a values of compound **27a** over the pH range of 2.0-10.5 in 0.1 M KCl at 25□.

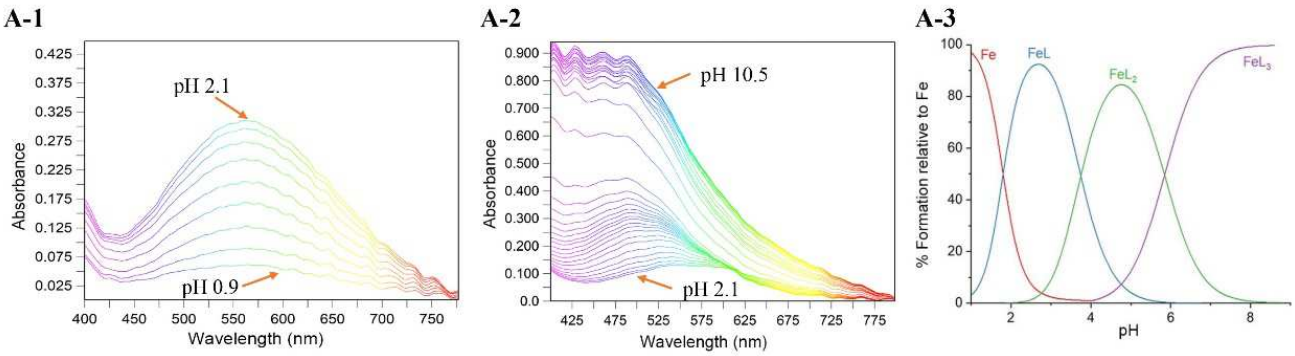

Fig. **3**. The pH-dependent UV spectra of compound **27a**. **A-1**. The pH-dependence of the spectrum of compound **27a** in the presence of Fe^{3+} over the pH range 0.9-2.1 in 0.1 M KCl at 25□, [Fe^{3+}] = 1.0 μM, [**27a**] = 1.1 μM. **A-2**. The pH-dependent spectra of compound **27a** in the presence of Fe^{3+} over the pH range 2.1-10.5 in 0.1 M KCl at 25□, [Fe^{3+}] = 1.0 μM, [**27a**] = 5.0 μM. **A-3**. Speciation plot of Fe^{3+}/ **27a** as measured by the percentage formation relative to $[iron^{(III)}]_{total}$ as a function of pH. This plot was calculated from the affinity constants reported in **Table 1** and the $iron^{(III)}$ hydrolysis constants were as follows: FeOH = -2.563, $Fe(OH)_2$ = -6.205, $Fe(OH)_3$ = -15.1, $Fe_2(OH)_2$ = -2.843, $Fe_3(OH)_4$ = -6.059, and $Fe(OH)_4$ = -21.883.

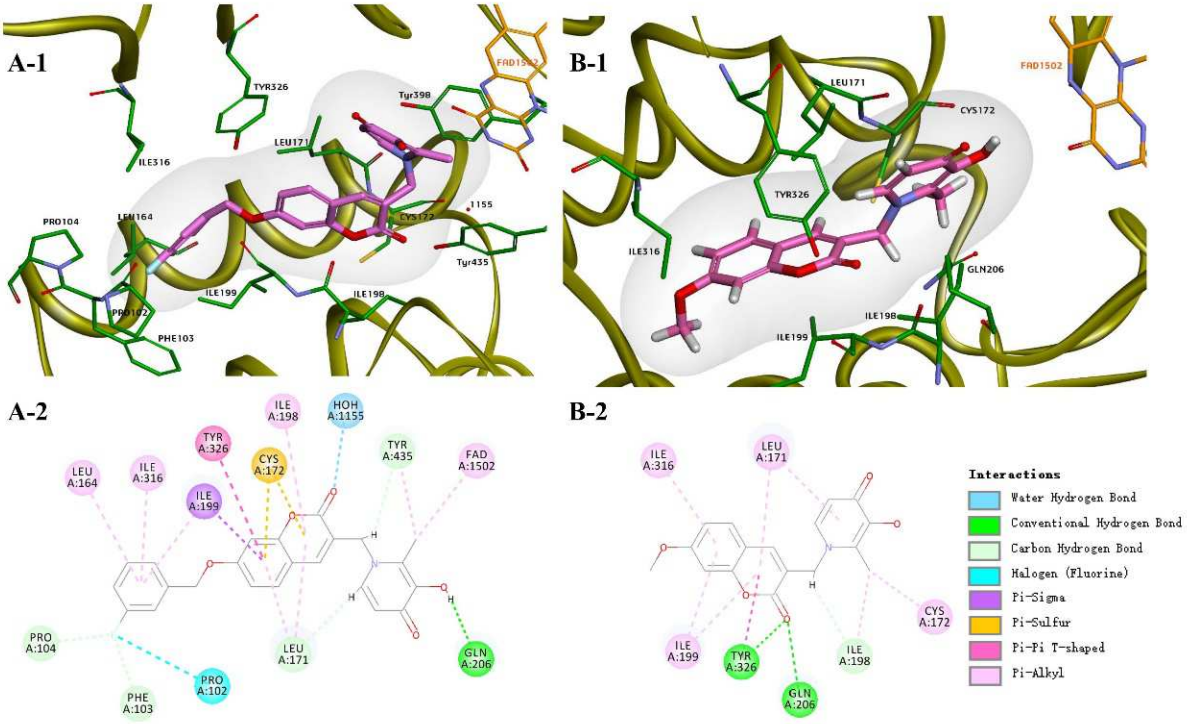

Fig. 4. Best docking poses of inhibitor **27a** and **13a** at the active site of MAO-B. The most relevant interacting residues are presented in green carbons polytube, FAD cofactor is shown as orange carbons polytube and ligands as pink carbons polytube. **A-1**, **B-1**. The 3D interaction diagram of **27a** and **13a** with MAO-B. **A-2**, **B-2**.The planar interaction diagram of **27a**, and **13a** with MAO-B.

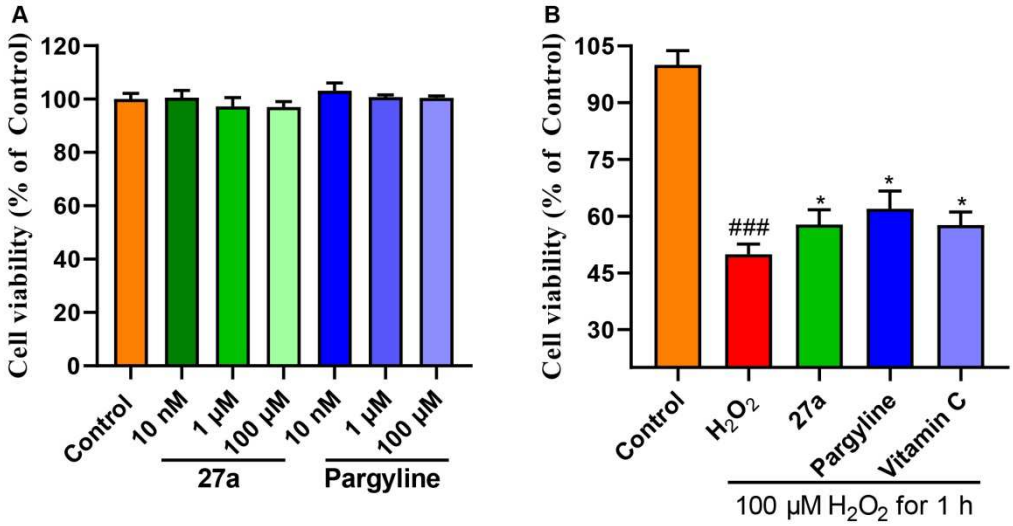

Fig. 5. Cytotoxicity and cytoprotective effects of compound **27a** on U251 cells. **A.** Cytotoxic activity after 24 h incubation with **27a** or pargyline at 10 nM, 1 µM and 100 µM on U251 cells. **B.** Cytoprotective effects of **27a** against H_2O_2-induced cell death on U251 cells. Cell viability was measured by MTS assay and data were expressed as a percentage of viable cells (referred to control). $^{###}P < 0.001$ vs. the control group. $^{*}P < 0.05$ vs. the H_2O_2 group treated with 100 µM of H_2O_2 for 1 h.

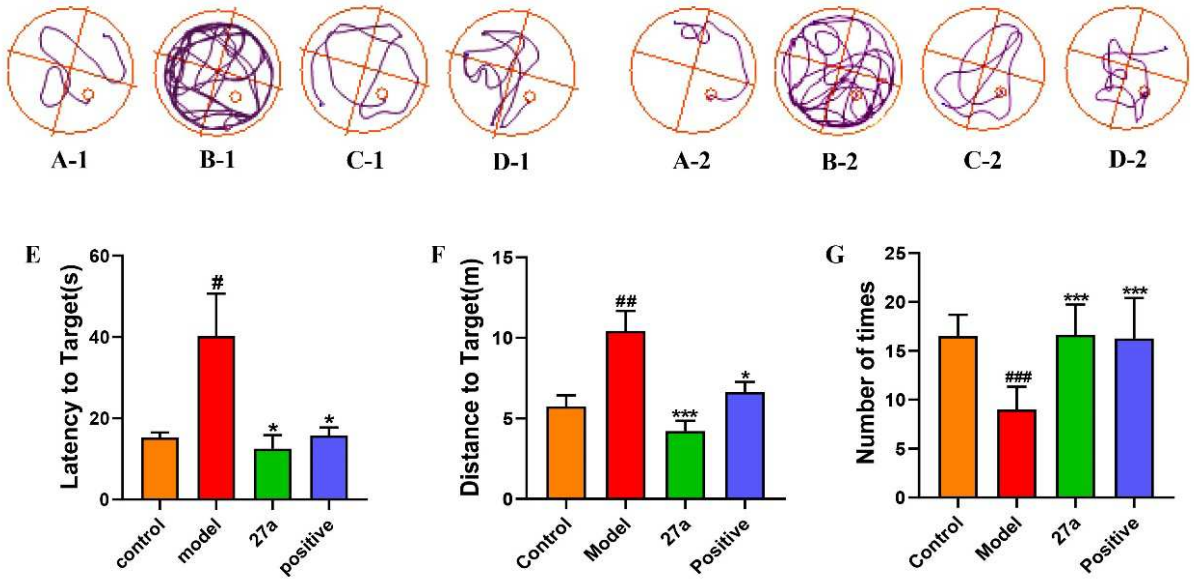

Fig. 6. Anti-AD effects of intraperitoneal injection of pargyline (10 mg·kg^{-1}), **27a** (10 mg·kg^{-1}), on scopolamine-induced cognitive impairment in ICR mice determined by the Morris water maze test. The trajectories of mice were shown as the control (**A1-2**), model (**B1-2**), **27a** (**C1-2**), and pargyline (**D1-2**) groups. **E**. The latency to target. **F**. The distance to the target. **G**. The number of times enter target quadrant. Data were presented as the mean ± SEM (n = 8; $^{\#}p < 0.05$, $^{\#\#}$p< 0.01, $^{\#\#\#}$p< 0.001, Control group vs. scopolamine model group; *p < 0.05, **p< 0.01, ***p< 0.001, **27a** or pargyline group vs. scopolamine model group).

Highlights:

A series of hydroxypyridinone-coumarin hybrids were designed and synthesized;

Most of the hybrids displayed excellent iron ion chelating effects;

Compounds **13a** and **27a** exhibited significant MAO-B inhibitory activity;

Compound **27a** showed good cytoprotective activity on U251 cells;

27a ameliorated the cognitive dysfunction of scopolamine-induced AD mice.